Climate
of the Past

Multi-century cool- and warm-season rainfall reconstructions for Australia's major climatic regions

Mandy Freund[1,2,3]**, Benjamin J. Henley**[1,2]**, David J. Karoly**[1,2]**, Kathryn J. Allen**[4]**, and Patrick J. Baker**[4]

[1]School of Earth Sciences, University of Melbourne, Melbourne, 3010, Australia
[2]ARC Centre of Excellence for Climate System Science, University of Melbourne, Melbourne, 3010, Australia
[3]Australian-German Climate and Energy College, University of Melbourne, Melbourne, 3010, Australia
[4]School of Ecosystem and Forest Sciences, University of Melbourne, Richmond, Victoria, 3121, Australia

Correspondence to: Mandy Freund (mfreund@student.unimelb.edu.au)

Abstract. Australian seasonal rainfall is strongly affected by large-scale ocean–atmosphere climate influences. In this study, we exploit the links between these precipitation influences, regional rainfall variations, and palaeoclimate proxies in the region to reconstruct Australian regional rainfall between four and eight centuries into the past. We use an extensive network of palaeoclimate records from the Southern Hemisphere to reconstruct cool (April–September) and warm (October–March) season rainfall in eight natural resource management (NRM) regions spanning the Australian continent. Our bi-seasonal rainfall reconstruction aligns well with independent early documentary sources and existing reconstructions. Critically, this reconstruction allows us, for the first time, to place recent observations at a bi-seasonal temporal resolution into a pre-instrumental context, across the entire continent of Australia. We find that recent 30- and 50-year trends towards wetter conditions in tropical northern Australia are highly unusual in the multi-century context of our reconstruction. Recent cool-season drying trends in parts of southern Australia are very unusual, although not unprecedented, across the multi-century context. We also use our reconstruction to investigate the spatial and temporal extent of historical drought events. Our reconstruction reveals that the spatial extent and duration of the Millennium Drought (1997–2009) appears either very much below average or unprecedented in southern Australia over at least the last 400 years. Our reconstruction identifies a number of severe droughts over the past several centuries that vary widely in their spatial footprint, highlighting the high degree of diversity in historical droughts across the Australian conti-

nent. We document distinct characteristics of major droughts in terms of their spatial extent, duration, intensity, and seasonality. Compared to the three largest droughts in the instrumental period (Federation Drought, 1895–1903; World War II Drought, 1939–1945; and the Millennium Drought, 1997–2005), we find that the historically documented Settlement Drought (1790–1793), Sturt's Drought (1809–1830) and the Goyder Line Drought (1861–1866) actually had more regionalised patterns and reduced spatial extents. This seasonal rainfall reconstruction provides a new opportunity to understand Australian rainfall variability by contextualising severe droughts and recent trends in Australia.

1 Introduction

Australia's climate varies between extreme states of severe dry conditions and devastating wet episodes affecting large areas of the continent (Nicholls et al., 1997). Shaped by high variability and persistence, floods, heat waves and droughts, Australia is highly vulnerable to changes in the climate system. One reason for the diversity in climate states is the influence of, and interactions among, large-scale ocean–atmosphere modes of variability. These include the El Niño–Southern Oscillation (ENSO), the Indian Ocean Dipole (IOD), the Southern Annular Mode (SAM), and atmospheric characteristics such as the strength and location of the subtropical ridge (STR) and the presence of atmospheric blocking (BLK). Critically, these tropical and extra-tropical modes of variability operate at and across different tempo-

ral scales and their individual and interacting influences have strong – and diverse – seasonal and regional effects on Australia's climate (Cai et al., 2014; Drosdowsky, 1993; Larsen and Nicholls, 2009; Maher and Sherwood, 2014; McBride and Nicholls, 1983; Oliveira and Ambrizzi, 2016; Ummenhofer et al., 2011; Wang and Hendon, 2007; Watterson, 2009, 2011).

Over the 20th century many regions in Australia have experienced prolonged pluvial and drought periods that are documented in the gridded, instrumental records starting in 1900. The Federation Drought (1895–1903) was one of the first multi-year periods of below average rainfall since European instrumental data collection began in Australia. There were also pronounced rainfall deficits during the World War II Drought (1939–1945) and the Millennium Drought (1997–2005), with devastating effects on regional agriculture and the broader economy (van Dijk et al., 2013).

In addition to these discrete drought events, there have also been a number of trends observed in Australian rainfall in recent decades. While there has been a general decrease in rainfall, particularly across southern Australia, these changes appear to have strong seasonal and regional components. For example, rainfall has declined in autumn across southern Australia (Larsen and Nicholls, 2009; McBride and Nicholls, 1983; Murphy and Timbal, 2008; Timbal et al., 2006), in the southwest during winter (Allan and Haylock, 1993; Cai and Cowan, 2008; Hope et al., 2009) and in southeast Queensland during summer (Smith, 2004; Speer et al., 2009). At the same time, regions in the north have received increasing rainfall (Feng et al., 2013; Taschetto and England, 2009; Wardle, 2004). The Millennium Drought, observed most severely in southwestern and southeastern Australia, was predominately due to deficits in cool-season rainfall (Verdon-Kidd and Kiem, 2009).

Given the presence of decadal (or longer) variability in the known climate drivers, short observational records are unlikely to provide a reliable estimate of the full extent of natural variability in Australia's climate system. In building a picture of the future likelihood of observed late 20th century trends continuing and the underlying likelihood of prolonged drought, it is essential that we understand the longer-term climatic context and its sources of variability. Palaeoclimate data can provide a unique window into long-term rainfall variability and emerging spatial and temporal trends. Such knowledge has practical applications for water resources management, seasonal forecasting, future climate predictions and potential to evaluate simulated past climate variations.

There have been a number of palaeoclimate reconstructions of hydrological variables in Australia (Allen et al., 2015; Cullen and Grierson, 2008; Gallant and Gergis, 2011; Gergis et al., 2011; Heinrich et al., 2009; Lough et al., 2015). Palmer et al. (2015) recently introduced the Australia and New Zealand Drought Atlas (ANZDA), using the approach developed for Asia (Monsoon Asia Drought Atlas (MADA) (Cook et al., 2010)), Europe (Old World Drought Atlas (OWDA) (E. R. Cook et al., 2015)) and North America by Cook et al. (2010). The ANZDA reconstructs the past 500 years of the Palmer Drought severity index (PDSI) for a $0.5° \times 0.5°$ grid over eastern Australia and New Zealand using a network of 176 tree-ring records and one coral record. Each of these reconstructions has advanced our knowledge of hydroclimatic variability at the bi-seasonal or annual scale for specific regions of Australia. To date, however, none have performed bi-seasonal reconstructions for the entire Australian continent.

The network of palaeoclimate proxies in Australia prior to the instrumental period is much sparser than for other regions such as Eurasia and North America. However, the strong links between large-scale remote climate drivers and Australian climate mean that remote proxies can contain a useful climate signal. Several recent studies have used remote teleconnections and climate drivers to obtain skilful reconstructions (Palmer et al., 2015; Tozer et al., 2016; Vance et al., 2015). In this study, we introduce a new method to reconstruct regional rainfall by systematically relating instrumental rainfall and proxy information to remote climate influences. We utilise a more dynamically focused methodology driven by dynamical relationships to include remote proxies and maximise the skill and widespread utility of our reconstructions of Australian rainfall.

Rainfall variations over the Australian continent show a large degree of spatial coherence at seasonal and longer time steps, due to the relatively simple terrain geometries and orography. The Climate Change in Australia report (CSIRO and Bureau of Meteorology, 2015) applied a regionalisation scheme to define eight natural resource management (NRM) regions with similar climatic and biophysical features. The NRM clusters and their abbreviations are listed in Table 1 and shown on the map in Fig. 1. In this study, we use a diverse network of local and remote palaeoclimate proxies to perform a reconstruction of cool- and warm-season rainfall in these eight NRM regions of Australia.

The aims of this study are as follows:

1. To consolidate relevant hydroclimate-sensitive palaeoclimate records.

2. To assess the sensitivity of the palaeoclimate records to the influences of large-scale climate influences and test the stationarity of these relationships.

3. To exploit the sensitivity of palaeoclimate proxies to large-scale climate influences and develop skilful palaeoclimate reconstructions of seasonal rainfall in eight NRM regions for several centuries into the past.

4. To compare the occurrence of wet and dry periods in the past to those in the instrumental period to provide a longer-term context for recent observed events and trends.
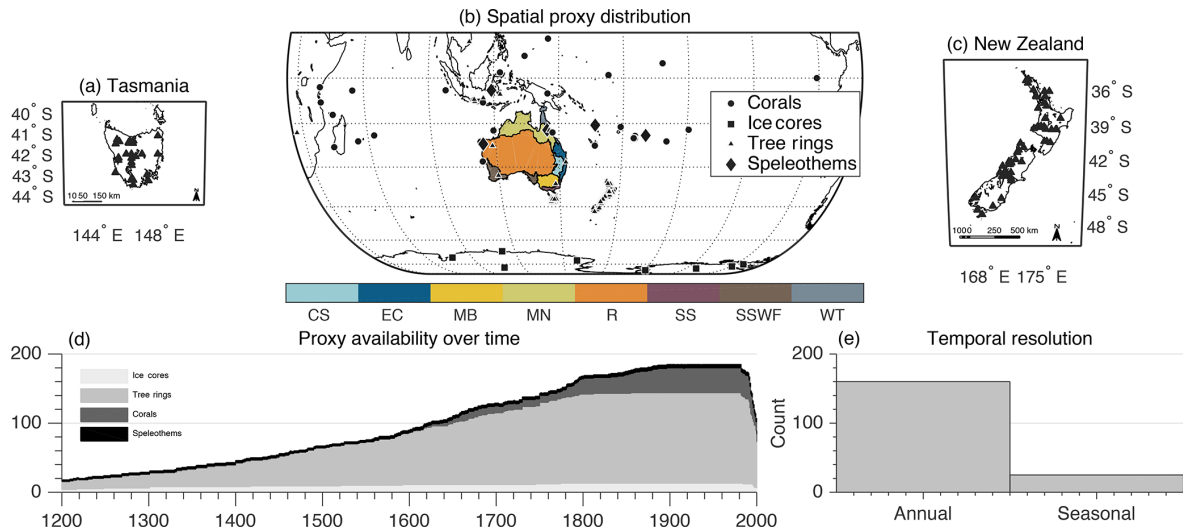
Figure 1. Overview of Southern Hemisphere multi-proxy network. **(a)** Spatial distribution of tree-ring sites in Tasmania **(b)** Spatial distribution of 202 individual proxy records by archive type; national resource management (NRM) clusters shown on Australian continent corresponding to abbreviations given in Table 1a. **(c)** Spatial distribution of tree-ring sites in New Zealand, **(d)** Record availability as a function of archive and time period covered, **(e)** Temporal resolution of the palaeoclimate records.

Our study is organised as follows: Sects. 2 and 3 describe the data and our methods, respectively. Section 4.1 presents a summary of the regional rainfall signature of modes of variability in the instrumental period. Section 4.2 presents the results of the reconstruction. In Sect. 4.3, we present an investigation of the trends, droughts and extreme years in a multi-centennial context, as well as a comparison to existing reconstructions. We finish by discussing these results and their broader implications in Sect. 5.

2 Data

2.1 Instrumental data

Our analysis is based on the Australian Bureau of Meteorology's gridded monthly precipitation dataset from the Australian Water Availability Project (AWAP) (Jones et al., 2009). The monthly AWAP dataset is based on precipitation anomalies generated from varying number of station observations using the Barnes successive-correction (Koch et al., 1983) and a three-dimensional smoothing spline interpolation (Hutchinson, 1995). Seasonal and regional averages are computed from the gridded observational dataset at its highest spatial resolution of $0.05° \times 0.05°$ for the period 1900–2015. The eight natural resource management (NRM) regions reflect a broad pattern of large-scale rainfall variability but may not capture finer-scale patterns.

We also use several climate indices to link climate drivers with Australian rainfall (Table 1a) that have previously been used to characterise the relationship between rainfall and large-scale drivers (Risbey et al., 2009). Computation of the individual climate indices strictly follows the descriptions in

references given in Table 1. The indices describe tropical influences (El Niño–Southern Oscillation (ENSO) and Indian Ocean Dipole (IOD/DMI); Saji et al., 1999) as well as extratropical drivers (Southern Annular Mode, SAM), the intensity and position of the subtropical ridge strength (STRI and STRP, Drosdowsky, 1993) and atmospheric blocking (BLK) (Pook and Gibson, 1999). ENSO is described by multiple indices, each of which relates to a different aspect of the coupled ocean–atmosphere mode. Here we use indices that are related to sea surface temperatures anomalies in the eastern Pacific (NCT) and the western Pacific (NWP) (Ren and Jin, 2011), the Southern Oscillation index (SOI) that measures the atmospheric component of ENSO, and the effects of central Pacific type events denoted by the ENSO Modoki index (EMI) (Ashok et al., 2007).

2.2 Palaeoclimate data

A palaeoclimate network of 185 individual records is compiled for the Southern Hemisphere (Fig. 1a). The multi-proxy network includes local and remote sites from a broad area that are related either directly or teleconnected to Australian climate (Fig. 1a). The majority of the records used are derived from the underlying network of the recently developed Australia and New Zealand Summer Drought Atlas (ANZDA) (Palmer et al., 2015) and the Ocean2k project, which is part of the PAGES (Past Global Changes) programme (Neukom and Gergis, 2012; Tierney et al., 2015). The entire network includes 131 tree-ring records from the Australasian Pacific area, 36 coral-derived records from the tropical Pacific and Indian oceans, and five speleothem-derived records. In addition, 13 records derived from Antarc-

Table 1. Summary of climate drivers, regions and droughts used in this study. (a) Climate indices and references for computational information; (b) mean, minimal and maximal seasonal contributions to annual rainfall totals (in %) for natural resource management (NRM) regions of Australia; and (c) instrumental and historical droughts.

(a) Climate Indices			(b) NRM Regions			(c) Droughts	
Climate index	Name	Ref	Region Abbrev.	Region name	Annual rainfall Cool: C; warm: W Avg (min–max)	Drought name	Period
SOI	Southern Oscillation index	BOM	MN	Monsoonal North	C: 10 % (5–25 %) W: 90 % (75–95 %)	Millennium Drought	1997–2009
NCT	Niño Cold Tongue index	Ren and Jin (2011)	WT	Wet Tropics	C: 18 % (7–39 %) W: 82 % (61–93 %)	World War II Drought	1935–1945
NWP	Niño Warm Pool index	Ren and Jin (2011)	EC	East Coast	C: 33 % (14–62 %) W: 67 % (38–86 %)	Federation Drought	1895–1903
EMI	El Niño Modoki index	Ashok et al. (2007)	CS	Central Slopes	C: 37 % (14–66 %) W: 63 % (34–86 %)	SE Drought	1836–1845
BLK	Blocking index	Pook and Gibson (1999)	MB	Murray Basin	C: 56 % (35–77 %) W: 44 % (23–65 %)	Goyder Line Drought	1861–1866
STRI	subtropical ridge intensity	Drosdowsky (1993)	SSWF	Southern and South-western Flatlands	C: 72 % (43–87 %) W: 28 % (13–57 %)	MD Basin Drought	1797–1805
STRP	subtropical ridge position	Drosdowsky (1993)	SS	Southern Slopes	C: 56 % (44–66 %) W: 44 %(34–56 %)	Great Drought	1809–1814
DMI	Indian Ocean Dipole	Saji et al. (1999)	R	Rangelands	C: 32 % (9–55 %) W: 68 %(45–91 %)	Sturt's Drought	1809–1830
SAM	Southern Annual Mode	Marshall (2003)				Black Thursday	1849–1866
						Settlement Drought	1790–1793

tic ice cores are included, as they are related to relevant large-scale high-latitude drivers such as SAM (Tozer et al., 2016; Vance et al., 2015). All records in the network extend back to at least 1880 CE and the majority cover the past 250 years. No further data treatment has been applied other than the removal of non-climatic biological trends in tree-ring records using the signal-free method that preserves much of the medium-frequency variability (timescales of decades to a century) (Melvin et al., 2008) (see Table S1 in the Supplement for references and details). Approximately half the records extend back before 1600 CE. Twenty records extend back to 1200 CE or earlier (Fig. 1b). Within this network, 160 proxy records are annually resolved records and 25 are sub-annually resolved (derived from corals) (Fig. 1c). Sub-annually resolved records are binned into seasonal averages according to a warm (October–March) and cool season (April–September). Samples within the seasonal window (six consecutive months) are averaged onto a regular time grid of two samples a year, whereas the dating of annually resolved records follows the original author.

3 Methodology

3.1 Reconstruction

The ocean–atmosphere processes that influence Australia's hydroclimate have distinct, but variable, seasonal and geographical characteristics (Risbey et al., 2009). In this study,

we first consider the relationships between the selected climate indices and warm (October–March) and cool-season (April–September) rainfall in each NRM region. The influence of each driver is determined by linear correlation for the concurrent season only. We exclude lag relationships between each driver and rainfall, which are generally weaker (Risbey et al., 2009). Relationships between precipitation and ocean–atmosphere processes can vary in strength over time (Gallant et al., 2013). We therefore use moving correlation windows (window length = 30 years) to assess statistically significant ($p < 0.1$) correlations for temporal stability. A relationship is considered stable if the interquartile range of windowed correlations remains of the same sign for the entire period of overlap between the two data sets. This approach ensures not only that the climate drivers have an approximately time-stable relationship with rainfall but also allows some degree of variation in the strength of the teleconnection. The same procedure to test stability was applied to the relationships between each proxy record (as listed in Table S1) and each climate index (as listed in Table 1a). Only proxies with a significant and time-stable relationship with an index were used as predictors for NRM regions with a time-stable relationship between that same index and precipitation (Table S2).

We use a nested, composite-plus-scale (CPS) approach (Bradley and Jones, 1993; Tierney et al., 2015) to reconstruct regionally averaged rainfall for each NRM region. Our CPS

approach combines principal components of proxy records into regional composites based on a weighted averaging procedure. The weight, w, is determined by (1) the coefficient of determination between each record and its target during the common period (1900–1984) and (2) the significance of this relationship, $w = r^2(1 - p)$, where p denotes the p values of the correlation, similar to Tierney et al. (2015). The resulting composite is re-scaled to the mean and standard deviation during the calibration period. It should be noted that not all of the records strictly follow a normal distribution (Fig. S7 in the Supplement). Using a nested approach entails the calculation of multiple reconstructions, with each reconstruction, or nest, extending further back in time but including fewer proxies as the proxies successively drop out (Fig. 1b). Nests are spliced together to form a continuous reconstruction. Nests are spliced together, based on the most replicated nest (most number of records available at a given time), to form a continuous reconstruction. This process maximises the length of the final reconstruction and ensures all proxies meeting the selection criteria are used at each point in time. The common period of palaeoclimate records and instrumental data (1900–1984) is used for calibration and verification. During the common period, 60 % of the data are used for calibration (equal to 51 contiguous years) and the remaining 40 % (34 years) are used for verification. We assess the sensitivity of our reconstruction to different calibration and verification periods by shifting our calibration window of 51 years across the common period in steps of 5 years. These different, but not independent, calibration and verification periods are used to build an ensemble of seven reconstructions for the warm and cool seasons.

Each final regional rainfall reconstruction is evaluated against a set of skill metrics. The coefficient of determination ($R^2{}_c$), is a measure of variance explained by the reconstruction in the calibration period, and $R^2{}_v$ is the variance explained in the verification period. Further skill statistics include the reduction of error (RE) and the coefficient of efficiency (CE), which both indicate statistical skill by positive values (Cook et al., 1994). Further analysis is conducted on the skilful portion of the reconstruction (CE > 0). We report our best reconstruction as that which maximises the time-integrated RE.

3.2 Analysis

Linear trends in the warm and cool season from instrumental and reconstructed precipitation are compared by fitting a linear trend line to the time series in 30- and 50-year moving windows. All trends are normalised by the maximum occurrence across each region and presented in histograms. All trend calculations are based on overlapping moving windows with a 1-year time step.

We investigate multi-year instrumental and historical periods of extremely low rainfall. During the instrumental period, three major droughts are assessed. These are the Mil-

lennium (1997–2009), World War II (1935–1945) and Federation droughts (1895–1903). Since European settlement, seven historical droughts are often reported in historical and documentary records. These include the Settlement Drought (1790–1793), the Murray Darling Basin Drought (1797–1805), the Great Drought (1809–1814), Sturt's Drought (1809–1830), Southeast Australia Drought (1836–1845), the Black Thursday Drought (1849–1866) and the Goyder Line Drought (1861–1866) (Helman, 2009). Details are provided in Table 1c.

We evaluate historical periods of drought by calculating seasonal and annual rainfall deciles based on the entire length of available data. For instrumental data, deciles are relative to the 1900–2014 long-term climatology, while reconstructed rainfall deciles include all positively verified years. The extended reconstruction includes all verified reconstructed years up to 1984, extended for the most recent 30 years of instrumental data up to 2014. The individual duration of deciles therefore depends on the time interval covered by each individual drought, as given in Table 1c. It is important to note that deciles deliver quantitative statements only in conjunction with a baseline period and duration, which may differ (example of different baseline periods Fig. S6). Resulting deciles are then categorised into highest on record, very much above average (10), above average (8–9), average (4–7), below average (2–3), very much below average (1) and lowest on record.

Drought durations are a challenge to compare using a decile-based approach alone. We therefore apply the concept of "drought–depth–duration" (DDD), following Fiddes and Timbal (2017) and Timbal and Fawcett (2013) to compare droughts of different duration. We present the percentage reduction below the long-term average of dry episodes ranging from 1 to 10 years. Our seasonal rainfall reconstruction uses the long-term average of the entire reconstruction as the baseline and presents the drought depth duration as the percentage reduction below this long-term average.

Ranking the seasonal rainfall totals in ascending order identifies extreme dry and wet years. The 10 highest and lowest years in the best reconstruction are reported in Table 2. As above, to provide a long-term context, the 10 driest and wettest years during the extended period (both the instrumental and the reconstruction periods) are identified.

In addition to pure statistical verification, we compare our results to other studies that have used historical documentary records and palaeoclimate archives to describe or reconstruct past hydroclimatic variability. Data from other studies with bi-seasonal resolution are averaged into the same warm and cool seasons used as the basis for reconstructions in this study. Annually resolved data are compared to both seasons. Single location records are compared to each of our regions. For the ANZDA (Palmer et al., 2015), area averages of the NRM clusters are extracted for comparison with the NRM regions.
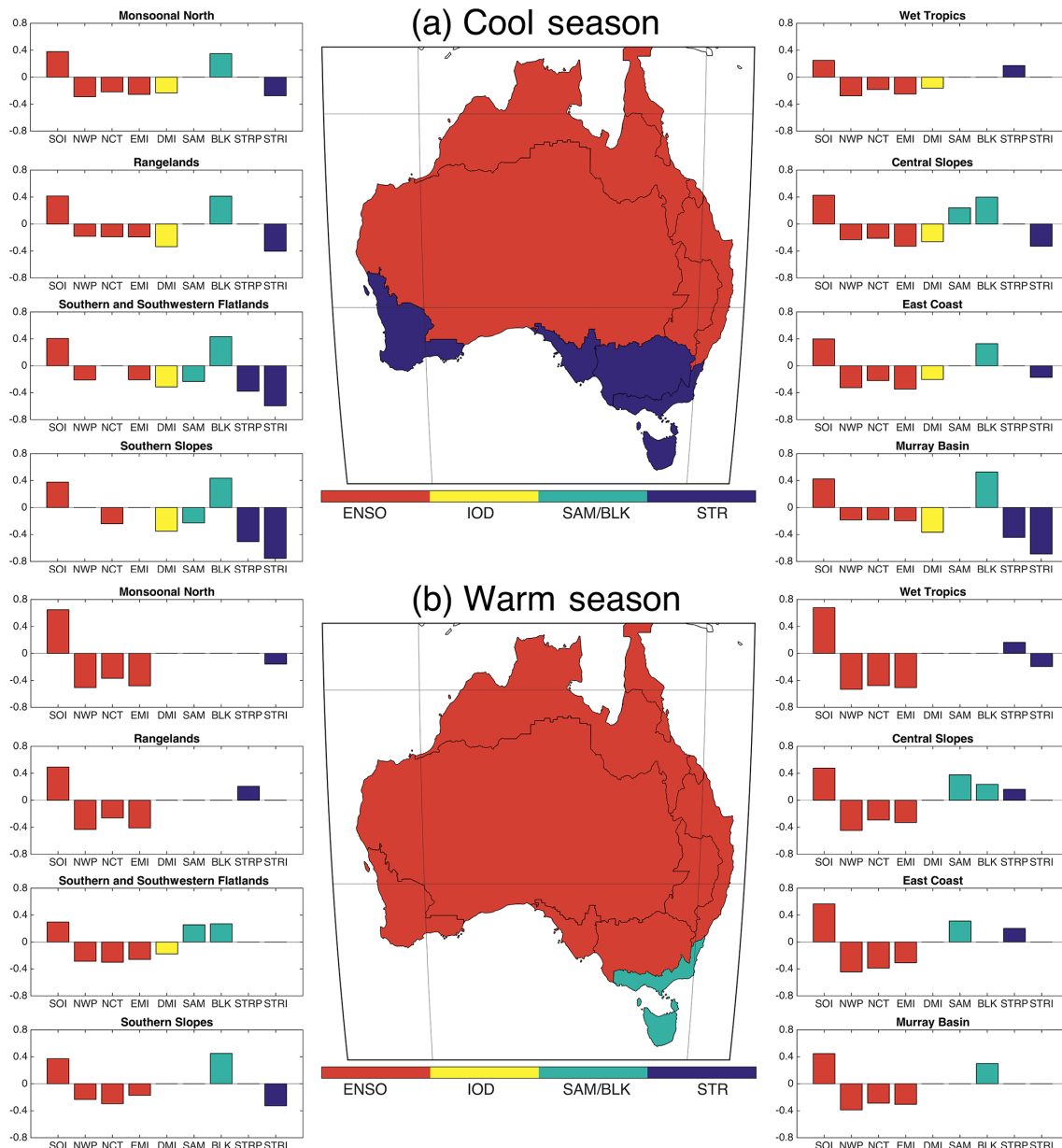
Figure 2. NRM regions and their dominant climate influences on **(a)** cool- and **(b)** warm-season rainfall. Centre maps show the climate driver with the highest correlation to seasonal precipitation according to the NRM regions. The drivers are summarised into four major categories: ENSO, IOD, SAM/BLK and STR (see Table 1a). Individual correlations between regional rainfall and each climate driver index are given in surrounding bar plots. Only significant correlations exceeding the 10 % significance level are shown.

4 Results

4.1 Influence of climate drivers on regional rainfall

The influence of climate drivers on rainfall variability across the NRM regions is significant and widespread. The influence of ENSO stands out across the tropical north and subtropical regions for both warm and cool seasons (Fig. 2a and b). Indeed, ENSO explains the greatest proportion of low-latitude rainfall variance (up to 44 %) during the peak-

intensity season (warm season) in the Wet Tropics. The dominant effect of ENSO decreases along a north–south gradient, with multiple-drivers becoming more important in the south. In southwest and southeast Australia (Flatlands, Southern Slopes, Murray Basin) the influence of mid-latitude pressure systems encapsulated by SAM and atmospheric blocking (BLK) increases. This north–south gradient is stronger during the cool season. In southern Australia (Southern Slopes and the Murray Basin), where cool-season rainfall dominates, the strength and positive influence of the subtrop-

Table 2. Extreme years. Summary of the 10 driest and wettest seasons for each NRM region for different baselines. Different baselines refer to the instrumental period (Instru: 1900–2014) and the extended reconstruction period (Pre-Instru: 1200–2014). Years highlighted in bold are among the 10 highest/lowest values for the entire reconstruction and instrumental period and therefore referred as extreme. Note the reconstruction period starts for verified periods only and differs for regions and seasons.

Region	Extreme	Period	Warm season	Cool season
CS	Driest	Instru	**1902, 1919, 1930, 1951, 1941**, 1901, 1905, 1900, 1918, 1942	**1994**, 1982, 2002, 1941, 1959, 1932, 1972, 1940, 1929, 1902
		Pre-Instru	**1433, 1868, 1791, 1391, 1431**, 1833, 1542, 1695, 1386, 1692	**1896, 1305, 1607, 1535, 1623, 1521, 1569, 1530, 1380**, 1502
	Wettest	Instru	**2011, 1970, 1962, 1971, 1950, 1983, 1910, 2010, 1974**, 1973	**1998, 1983, 1920, 1988, 1990**, 1950, 1921, 1915, 1938, 1952
		Pre-Instru	**1644**, 1618, 1662, 1748, 1716, 1370, 1613, 1739, 1628, 1733	**1557, 1878, 1796, 1513, 1745**, 1212, 1206, 1764, 1405, 1432
EC	Driest	Instru	**1919**, 1942, 1905, 1945, 1936, 1901, 1937, 1902, 2006, 1992	**1946, 1918, 2004, 1994**, 1951, 1960, 1968, 1965, 1982, 1991
		Pre-Instru	**1386, 1383, 1413, 1807, 1428, 1542, 1391, 1499, 1474**, 1385	**1800, 1716, 1681, 1679, 1871, 1860**, 1760, 1714, 1680, 1758
	Wettest	Instru	**2010, 1970, 1974, 1971, 1975, 1973**, 1960, 1962, 1910, 1955	**1983, 1988, 1989, 1998, 1931**, 1912, 1913, 1924, 1920, 1949
		Pre-Instru	**1752, 1740, 1732, 1875**, 1627, 1731, 1602, 1753, 1743, 1742	**1728, 1820, 1726, 1769, 1879**, 1770, 1786, 1742, 1787, 1833
MB	Driest	Instru	**1902, 1900**, 1905, 1901, 1931, 1918, 1925, 1932, 1963, 1951	**1982, 1976, 1994, 1966, 2006, 1980**, 2002, 1925, 1936, 1914
		Pre-Instru	**1540, 1691, 1251, 1695, 1542, 1485, 1543, 1394, 1900**, 1899	**1778, 1779, 1811, 1838**, 1480, 1817, 1885, 1481, 1607, 1780
	Wettest	Instru	**2010, 1992, 2011, 1950**, 1973, 1971, 1955, 1983, 1970, 1956	**1915, 1916**, 1955, 1973, 1956, 1970, 1974, 1968, 1975, 1917
		Pre-Instru	**1694, 1668, 1588, 1751, 1340, 1750**, 1298, 1795, 1693, 1732	**1572, 1516, 1706, 1495, 1649, 1532, 1523, 1575**, 1537, 1721
MN	Driest	Instru	**1951, 1902, 1905, 1991**, 1935, 1919, 1989, 1965, 1918, 1953	**1926, 1931, 1930, 1935, 1932, 1933**, 1994, 2002, 1964, 1934
		Pre-Instru	**1896, 1761, 1837, 1838, 1899, 1814**, 1746, 1760, 1762, 1758	**1745, 1818, 1684, 1783**, 1878, 1667, 1658, 1760, 1808, 1900
	Wettest	Instru	**2010, 2000, 1973, 1999, 2008, 1950, 1976, 1998, 1975, 2003**	**2010, 2006, 1955, 1910, 1959, 2000, 1950, 1956, 1983**, 1974
		Pre-Instru	1893, 1720, 1887, 1886, 1731, 1879, 1870, 1802, 1722, 1805	**1694**, 1882, 1881, 1887, 1826, 1879, 1669, 1739, 1801, 1690
R	Driest	Instru	**1965**, 1964, 1905, 2004, 1951, 1963, 1912, 1925, 1902, 1953	**1925, 1940, 1976, 1902, 1994, 2002**, 1946, 1926, 1941, 1944
		Pre-Instru	**1745, 1746, 1607, 1872, 1611, 1696, 1683, 1698, 1760**, 1868	**1891, 1832, 1855, 1812**, 1838, 1817, 1849, 1888, 1868, 1862
	Wettest	Instru	**2010, 1999, 2000, 2011, 1979, 1980, 1973, 1978, 1976, 1975**	**1998, 2010, 1974, 1970, 1978, 1968, 1973**, 1992, 1933, 1904
		Pre-Instru	1664, 1673, 1886, 1855, 1720, 1690, 1735, 1672, 1663, 1633	**1879, 1825, 1826**, 1819, 1829, 1870, 1881, 1880, 1861, 1894
SS	Driest	Instru	**1919, 1963, 2006**, 1997, 1913, 2002, 2012, 1982, 1977, 1967	**1940, 1902, 1982, 1999, 1966**, 2008, 1937, 1977, 1967, 1987
		Pre-Instru	**1439, 1381, 1437, 1799, 1438, 1744, 1868**, 1818, 1413, 1433	**1855, 1865, 1888, 1887, 1817**, 1840, 1799, 1869, 1833, 1784
	Wettest	Instru	**2010, 1910, 1955, 1974, 1950**, 1930, 1992, 1948, 1956, 1988	**1961, 1960, 1974, 1958, 1975, 1962, 1973**, 1942, 1956, 1953
		Pre-Instru	**1890, 1731, 1398, 1372, 1894**, 1649, 1892, 1740, 1730, 1887	**1789, 1872, 1848**, 1774, 1871, 1759, 1810, 1750, 1859, 1843
SSWF	Driest	Instru	1951, 1975, 1905, 1965, 1930, 1990, 1963, 2004, 1949, 1900	**1957, 2006, 1914, 1976, 1940**, 1994, 1982, 2010, 2002, 1911
		Pre-Instru	**1814, 1445, 1610, 1559, 1536, 1449, 1223, 1255, 1247, 1297**	**1514, 1376, 1481, 1492, 1488**, 1550, 1494, 1459, 1555, 1509
	Wettest	Instru	**1999, 1914, 1916, 1933, 1938, 2005, 2011**, 1959, 1992, 1942	1931, 1915, 1917, 1909, 1907, 1927, 1908, 1910, 1942, 1920
		Pre-Instru	**1417, 1565, 1588**, 1340, 1427, 1586, 1245, 1649, 1218, 1239	**1871, 1603, 1370, 1470, 1367, 1605, 1612, 1759, 1368, 1808**
WT	Driest	Instru	**1982, 1905**, 1941, 1925, 1965, 1902, 1904, 1968, 1991, 1946	1967, 1953, 1965, 1966, 1968, 1915, 2008, 1923, 1991, 1997
		Pre-Instru	**1314, 1671, 1251, 1504, 1313, 1317, 1761, 1335**, 1305, 1433	**1607, 1251, 1495, 1391, 1540, 1584, 1608, 1536, 1284, 1223**
	Wettest	Instru	**2010, 1975, 1973, 1974, 1998**, 2000, 1976, 1971, 1910, 1917	**2006, 1989, 1990**, 1976, 1983, 1981, 1956, 1945, 1971, 1972
		Pre-Instru	**1469, 1752, 1886, 1467, 1678**, 1242, 1425, 1241, 1874, 1471	**1245, 1231, 1212, 1210, 1881, 1661, 1340**, 1413, 1228, 1209

ical ridge (STRP) is important. In southeastern Australia, the correlation between rainfall and the STRP is as strong as $r = 0.78$, highlighting the importance of the subtropical ridge on rainfall. Although the influence of the STRI dominates rainfall in these regions in the cool season, SAM, BLK and ENSO still have significant associations with mid-latitude rainfall (Fig. 2a). While conditions in the tropical Pacific have a strong influence on warm-season rainfall across the continent, the conditions in the IOD have mostly cool-season impacts, except in the Wet Tropics. These results are consistent with previous studies (e.g. Risbey et al., 2009).

4.2 The reconstruction

4.2.1 Reconstruction skill

Our reconstruction captures 30–60 % of seasonal rainfall variability across the regions. Skill statistics of the reconstruction (Fig. 3) show that the variance explained during the calibration period (1934–1984) is around 37 % (R^2_c [0.2–

0.5]) for the cool season and 34 % (R^2_c [0.2–0.6]) for the warm season (Fig. 3a and b). During the independent verification period (1900–1933), a slightly larger magnitude of variance is explained by the reconstruction, with about 46 % (R^2_v [0.2–0.6]) for the cool season and 48 % (R^2_v [0.3–0.6]) for the warm season. These high and stable proportions of variance captured by the reconstructions are found for both seasons. The RE and CE statistics are positive for all regions, indicating reconstruction skill for both seasons across Australia (Fig. 3a and b). Given that our reconstruction is based on a nested approach, with a varying set of proxies over time, we indicate in Fig. 3 the timeframe during which the individual reconstructions show reliable skill for each region and season. The years shown on each region for the R^2 panels (Fig. 3a, b, e, and f) indicate the earliest year in which the reconstruction exceeds half of its maximum skill; years shown on the RE and CE panels (Fig. 3c, d, g, and h) indicate the earliest year in which the RE and CE statistics remain positive, allowing for brief periods of negative skill, of duration
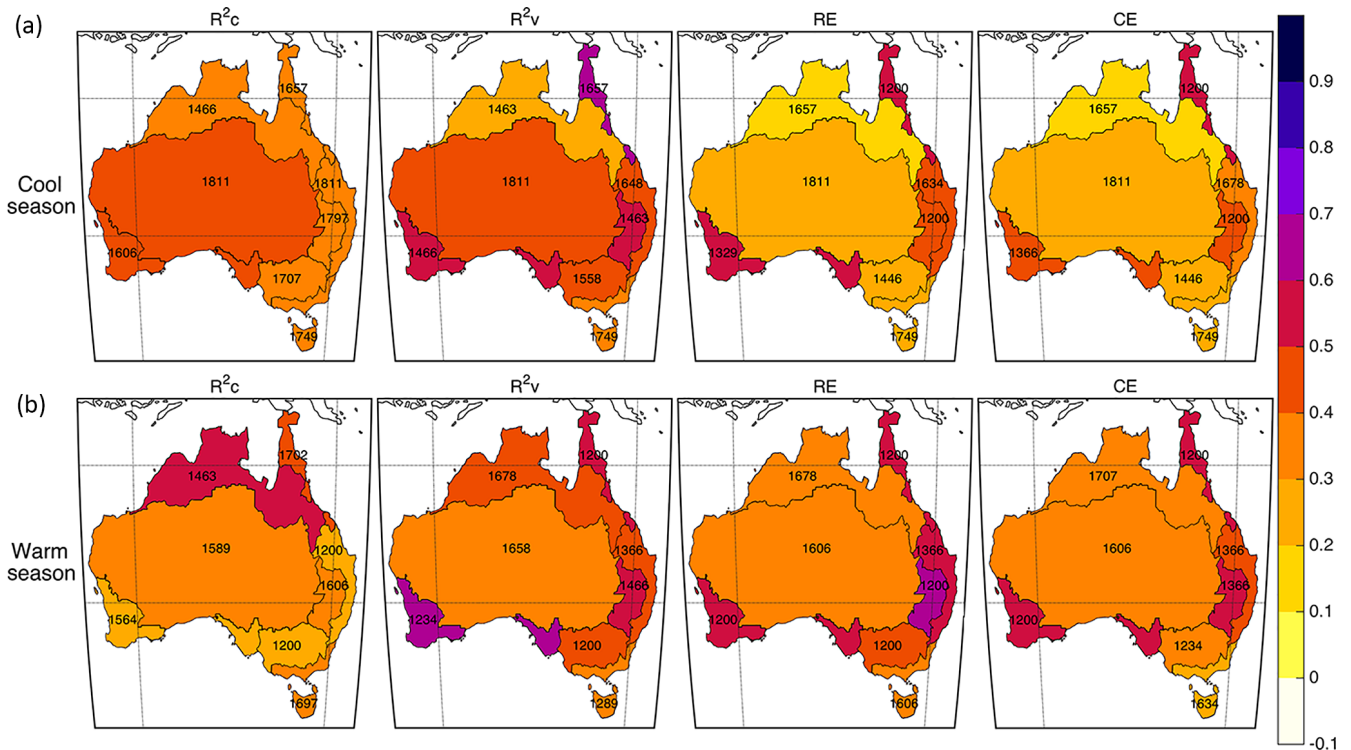
Figure 3. Maps of calibration and verification statistics for the NRM regions. Columns from left to right are variance explained in the calibration period (R^2_c), variance explained in the verification period (R^2_v), reduction of error (RE) and coefficient of efficiency (CE) statistics for both the cool season **(a)** and the warm season **(b)**. Statistics shown apply to the most replicated nest of the reconstruction. Numbers shown in each region indicate, for explained variance, the year in which R^2_c and R^2_v reduce to half of their maximum value, respectively; those for RE and CE indicate the year in which RE and CE remain positive, allowing for brief periods of negative skill of duration less than 5 years.

less than 5 years. The year shown on the CE plots indicates the earliest year for which the reconstruction is considered skilful (i.e. CE > 0).

During the cool season, the Central Slopes, Wet Tropics, and South and Southwestern Flatlands indicate the longest skilful (CE > 0) reconstructions, extending back to 1200, 1260 and 1366, respectively. The rainfall reconstruction in the Rangelands is only skilful back to 1811 and represents the shortest skilful reconstruction during the cool season. Most of south and southeastern Australia in the cool season can be reconstructed back to at least 1749 (Southern Slopes).

In the warm season, the Southern and Southwestern Flatlands, Wet Tropics, and Murray Basin warm-season reconstructions are skilful (CE > 0) for the longest period, extending back to 1200, 1200 and 1234, respectively. The warm-season rainfall reconstruction in the Monsoonal North has the shortest skilful reconstruction, back to 1707. Warm-season reconstructions for south and southeastern Australia indicate slightly longer periods of skill than the cool-season reconstructions.

4.2.2   Reconstruction time series

Seasonal time series of our reconstructed rainfall across Australia show high rainfall variability over the instrumental period (Fig. 4). Interannual and decadal-scale rainfall variability is well characterised by the reconstructions. For example, the pluvial periods in the mid-1950s and late 1970s during the warm season in the eastern regions (top three panels) are remarkably well reconstructed. Although different calibration and verification periods indicate some differences at interannual scales (grey shading), encouragingly, decadal variability is well represented by the ensemble. In particular, seasons which dominate the total rainfall are well captured in terms of their amplitude, for example the warm season in the Wet Tropics and cool season in the Murray Basin.

Decadal variability is evident in all warm- and cool-season reconstructions (Figs. 5, S2 and S3). At decadal timescales, both the warm and cool seasons show synchronous decades of enhanced/reduced rainfall across different regions. For example, the very dry warm seasons (Fig. S3) observed in the 1960s (Central Slopes, Murray Basin, Rangelands, Southern Slopes, Southern and Southwestern Flatlands, Wet Tropics) are also seen in the 1760s across similar regions (Central
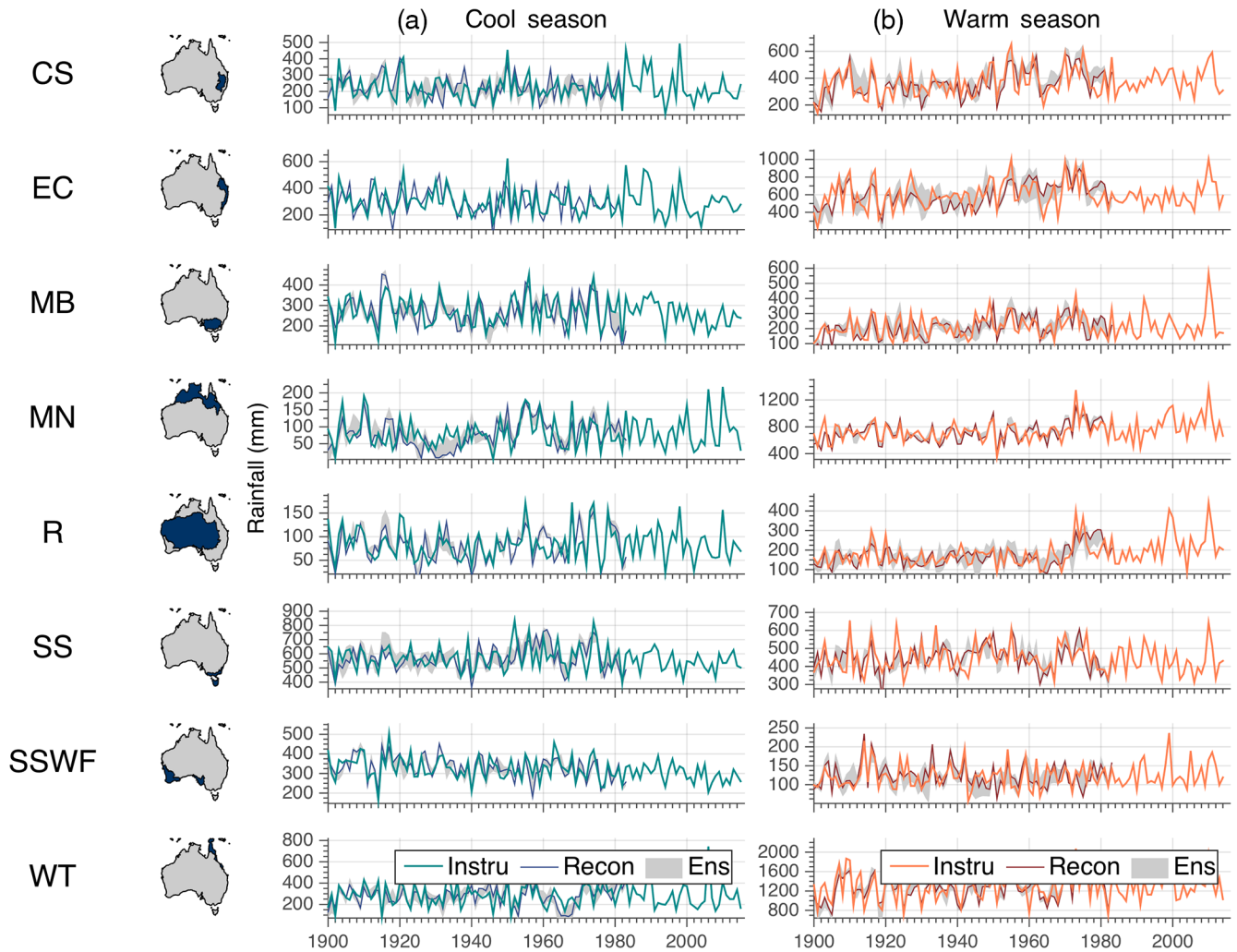
Figure 4. Australian regional rainfall reconstructions during the instrumental period (1900–2015). Reconstructed cool-season **(a)** and warm-season **(b)** rainfall is compared with the instrumental. Shaded in grey are uncertainty estimates based on the ensemble spread.

Slopes, Murray Basin, Monsoonal North, Southern Slopes, Southern and Southwestern Flatlands, Wet Tropics). During the 1740–1750s extreme wet conditions prevailed in southern and southeastern Australia. Rainfall during those 20 years was mostly above average for much of eastern Australia (Central Slopes, East Coast, Murray Basin). In the 1970s similar regions saw a decade of higher than normal warm-season rainfall (Central Slopes, East Coast, Rangelands, Wet Tropics). There seems to be no general pattern of prolonged decadal drought or pluvial conditions associated with specific regions in our reconstructions.

The magnitude of the warm-season pluvials during the 1970s and 1740–1750s are not anomalously high based on the cool-season reconstructions (Fig. S2). Only East Coast and Rangelands show similarly high rainfall amounts, while other regions show average or sightly drier conditions (Central Slopes). Most of the cool-season decadal trends show very distinct regional patterns. Wetter than normal conditions

in the 1870s are only evident in the Central Slopes and East Coast. Even geographically proximate regions such as the Murray Darling Basin region and the Southern Slopes show dissimilarities in terms of decadal-scale variability. Overall, warm-season rainfall seems to show slightly more concurrent decades across the regions than during the cool season.

To assess the degree to which the reconstructions are seasonally distinct, shaded areas in Fig. 5 highlight periods when the warm- and cool-season reconstructions are significantly correlated (30-year moving window, abs(correlation) > 0.5). There are a small number of periods during which the cool- and warm-season rainfall are in phase (positively correlated, shown in red) or out of phase (negatively correlated, shown in blue). However, for the most part, there is little dependence between the seasonal reconstructions. Although some regions show periods in which warm- and cool-season reconstructed rainfall are in phase, this feature is also present in some instances in the instru-
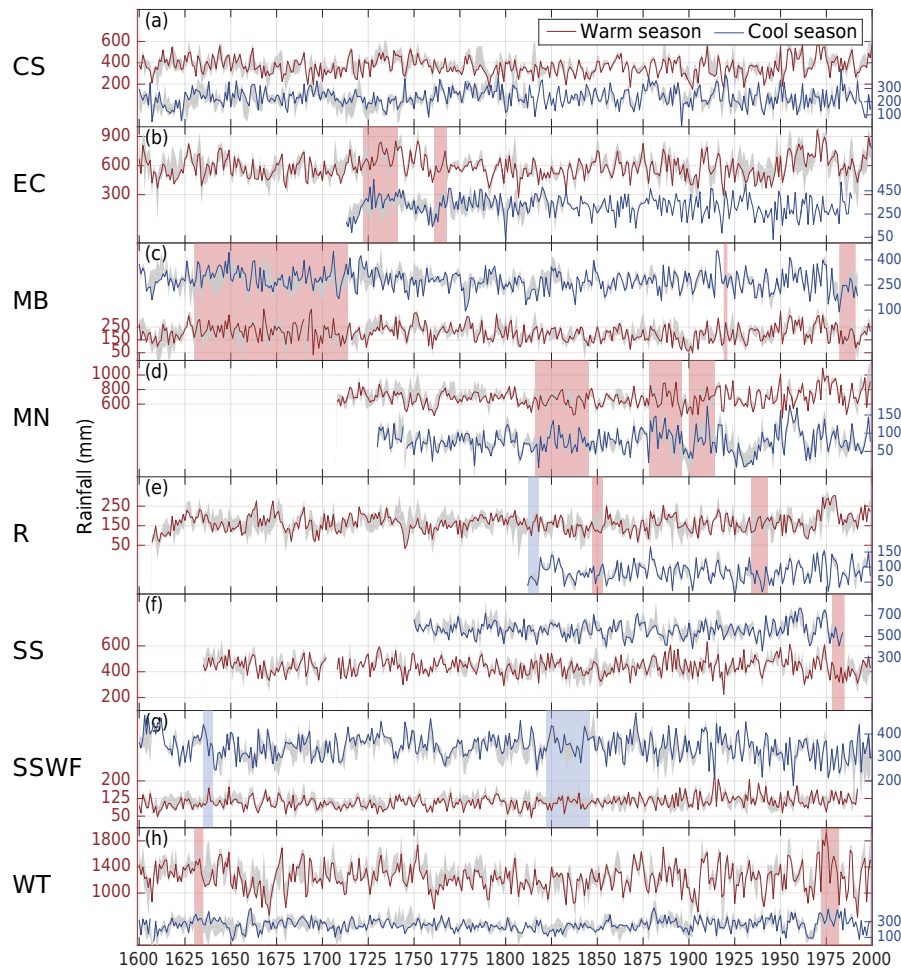
Figure 5. Australian regional rainfall reconstructions in cool and warm seasons. Regional reconstructions for warm- (red line) and cool-season rainfall (blue line) from 1600 to 1984, extended with instrumental data from 1985 to 2015. Note that multiple axes (warm-season rainfall according to left axis, cool season refers to right axis). Shaded in grey are uncertainty estimates based on the ensemble spread. Red and blue shaded periods indicate in-phase and out-of-phase relationships between the seasons based on windowed correlations (30 years)> 0.5.

mental period. For example, the 1720s and 1760s are periods in which East Coast warm- and cool-season rainfall are positively correlated. During these decades, there is a degree of synchronicity, meaning that reduced/increased rainfall in the cool season is accompanied by reduced/increased rainfall in the following warm season. From 1820–1840 cool- and warm-season rainfall in the Southern and Southwestern Flatlands is anti-correlated, indicating opposing seasonal rainfall totals. Rainfall in the late 1970s/1980s in the Murray Basin, Southern Slopes and Wet Tropics are examples of positive inter-seasonal correlations (Fig. 5c, f and h) in the instrumental period. Whilst some regions have short periods of synchronicity across seasons, this is observed across both the reconstruction and instrumental periods and the general pattern is one of seasonal independence.

4.3   Australian rainfall and drought in a multi-century context

4.3.1   Contextualising recent rainfall trends

Since the start of instrumental records in Australia, several major droughts and extended pluvial periods have been observed. Some influences can be regarded as temporary changes in the mean state due to, for example, natural decadal climate variability from the Interdecadal Pacific Oscillation (IPO; Henley et al., 2015, 2017). Other changes appear to be more strongly related to long-term changes in atmospheric circulation. These changes are spatially and temporally diverse, and strong interannual variability makes it hard to distinguish between low-frequency variability from externally forced long-term changes. Here we use our rainfall reconstructions to place recent observed trends in a long-term centennial context.

The histograms in Fig. 6 summarise all 30 and 50-year linear trends in the regional reconstructions and instrumental data over the period 1600–2014. The distributions of trends distinguish between pre-1970 variability (grey), trends since 1970 or 1950 (depending on the fitted trend length of 30/50 years; shown in light blue/red for cool/warm season) and the trend from the most recent 30 or 50 years. The regional reconstructions show recent tendencies towards drier cool seasons in the south (Murray Basin, Southern Slopes, Southern and Southwestern Flatlands) and wetter warm seasons in the north (Monsoonal North, Rangelands, Wet Tropics). The distribution of historical trends derived from the reconstructions are of a generally Gaussian distribution. Some trends starting after 1950/1970, including the most recent trend, are shifted towards the upper and lower quartile range of the pre-1950/1970 trends. Trends starting after 1950/1970, including the most recent trend (ending in 2014), appear unusual, but not unprecedented. In recent years, during the warm season, tropical regions in particular show a strong increase in rainfall. This is strongest in the Monsoonal North, followed by the Rangelands and Wet Tropics (Fig. S3). Some subtropical regions show a warm-season decrease in rainfall, strongest in the Southern Slopes, but again not unprecedented. All regions, except the Monsoonal North, show a decline in rainfall in the cool season during the most recent 30- and 50-year periods. This decline is most pronounced in the Southern Slopes, Southern and Southwestern Flatlands and the Murray Darling Basin. Cool-season rainfall, which contributes the majority of subtropical rainfall, has clear negative shifts in southern Australia, compared to earlier trends. In particular, cool-season rainfall in the Murray Basin saw declines over the last 30 and 50 years of the order of 90 mm.

4.3.2 Contextualising the spatial extent and intensity of past droughts

Extended periods of low rainfall have different characteristics in their temporal and spatial structure. The assessment of drought risk depends critically on the range of estimated natural variability. Here we assess the severity of major drought episodes using deciles across both instrumental (1900–2014) and multi-century reconstruction (1600–2014) periods. Our regional rainfall reconstruction comparisons here extend the time span of the instrumental record by a factor of 4, which enables us to view droughts such as the Millennium Drought in a very long-term multi-century context. Deciles based on different datasets, baselines and durations are shown in Fig. 7. Comparing the spatial pattern of the reconstructed droughts to the gridded and NRM region instrumental (AWAP) spatial patterns, our reconstruction depicts the intensity of the two drought events during the instrumental period quite well. The gridded and regional representation of the Millennium Drought is indicated as the lowest on record for parts of the Southern Slopes and the Murray Basin and very much below average for the East Coast and the

South and Southwestern Australia, in agreement with other studies (Cai et al., 2014; Gergis et al., 2011; Verdon-Kidd and Kiem, 2009). In the context of the full reconstruction period (1600–2014), the Millennium Drought remains the worst drought since 1749 in the Southern Slopes (observable too in Fig. 5f) and very much below average for East Coast, Murray Basin, and Southern and Southwestern Flatlands. In line with probability estimates for southeastern Australia by Gergis et al. (2011) and B. I. Cook et al. (2015), the 12-year period of the Millennium Drought is unprecedented for the Southern Slopes region. The rainfall reconstruction of the Murray Basin reveals that periods in the late 1700s and early 1800s and at the time of the Federation Drought are of similar or larger reductions in rainfall over a 12-year period (Fig. 5c). The Federation Drought period is also apparent in the Southern and Southwestern Flatlands reconstruction, along with other periods of rainfall reductions the late 1600s (see Fig. 5g).

The World War II Drought and the Federation Drought appear to be of somewhat similar character during the instrumental period in terms of their area and intensity (Fig. 7 gridded and NRM regional plots). Considering the last 400 years, the World War II Drought is a period of average rainfall for all regions except the Murray Basin, Central Slopes and East Coast. In contrast, the Federation Drought (1895–1903) is much higher in intensity and spatial coverage. In Fig. 7 we compare the Federation Drought during its instrumental period and full (including pre-instrumental) period. During the observational period (the latter part), the Federation Drought shows only slightly below average conditions. In the multi-century context, the Federation Drought shows a wider extent. Along the east coast (Central Slopes, East Coast), central parts (Rangelands, Murray Basin, Southern Slopes) and north Australia (Monsoonal North, Wet Tropics) the Federation Drought was very much below average and lowest on record for Monsoonal North and Murray Basin, respectively.

Historical droughts during the pre-instrumental period (Table 1c, Figs. 7 and S6), as documented mainly in southeastern Australia due to the concentration of European settlement there, are captured by the reconstruction. The Goyder Line Drought, Sturt's Drought and the Great Drought appear to have affected only certain distinct regions. The Settlement Drought shows regions clearly below average, especially coastal regions and the Murray Basin, similarly to Palmer et al. (2015) and Gergis et al. (2010). The representation in terms of affected regions aligns very well with historical reports (e.g. historical reports by Sturt or the definition of the Goyder Line). Most of the historical droughts have been below average in certain regions but none of these droughts appear to exceed the spatial extent and intensity of the three major instrumental-period droughts.
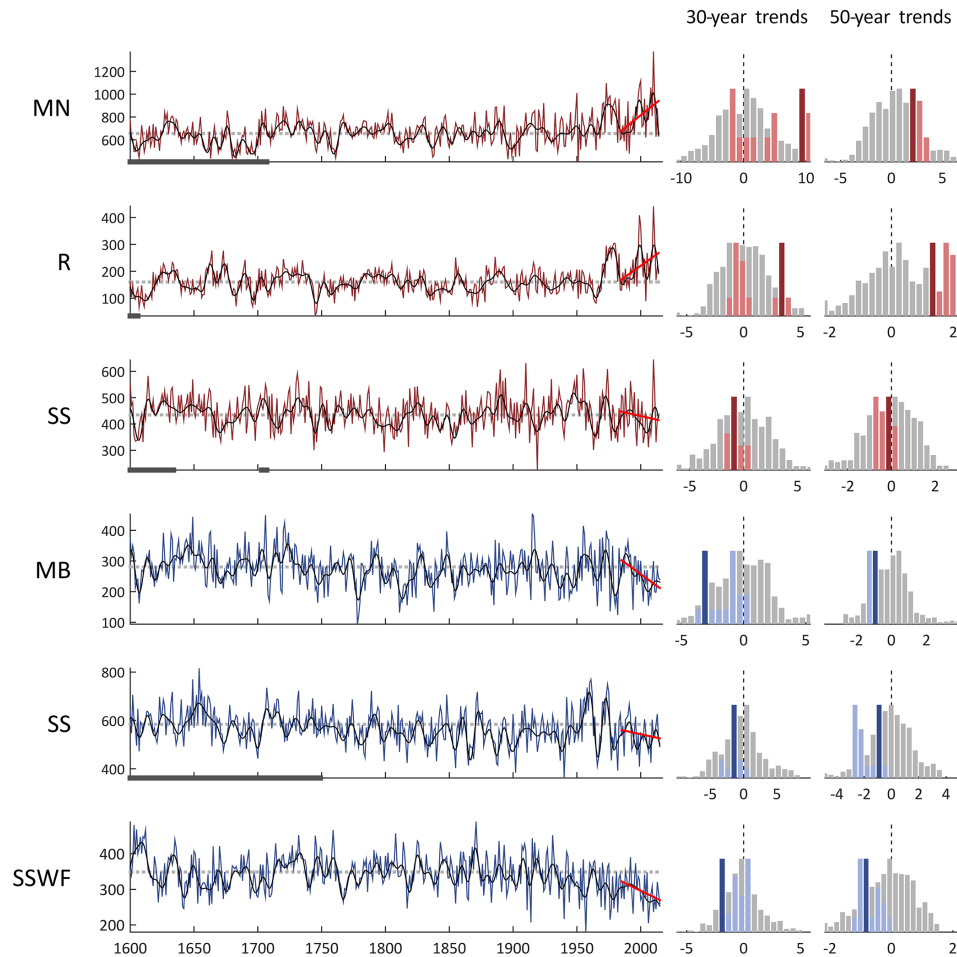
Figure 6. Contextualising recent observed trends in regional Australian rainfall. Left panels show regional rainfall reconstructions since 1600 for the warm (red) and cool season (blue) with the 10-year low-pass Chebyshev filtered series shown as a black line. Grey bars along the x axis denote non-verified periods for each reconstruction. Right panels show histograms of 30- and 50-year regional rainfall trends (mm yr^{-1}). Grey shaded bars indicate the full range of the trends prior to 1970 (for 30-year periods) and 1950 for 50-year periods. Light red/blue colouring highlights the trends since 1970 (for 30-year periods) or 1950 for 50-year periods. The dark coloured bars indicate the trend in the most recent period. Bar heights are normalised by the maximum occurrence for each region.

4.3.3 Contextualising the duration and seasonality of past droughts

We apply the concept of drought–depth–duration (DDD) to our reconstructions to further assess the duration and intensity of the different droughts (see Sect. 3.2 for details). The DDD plots provide a method to compare the temporal structure of drought periods. Additionally, our bi-seasonal reconstruction resolution provides an opportunity to investigate the seasonal nature of protracted droughts and therefore provides insight into their climatic influences and potential causes.

Using the DDD analysis we can categorise droughts into long- and short-term droughts and distinguish the primary season of the droughts. The Millennium Drought is among the worst droughts in terms of its duration across several of the NRM regions in southern and eastern Australia (Fig. 8, dark blue lines). In particular, during the cool season, the re-

duction in rainfall extends over very long periods for central and eastern regions (Central Slopes, East Coast and Murray Basin). By comparing short periods (2 < years) to longer periods (> 6 years) the Millennium Drought is revealed as a persistent drought, with its worse impacts being felt over the longer timeframe. The Murray Darling Basin Drought is predominately caused by cool-seasonal rainfall deficiencies over long periods, plus a slight accumulated rainfall deficit during the warm season in the Southern Slopes. The World War II Drought had similar cool-season rainfall reductions; however, the warm-season rainfall was also affected. These are similar to the findings of (Verdon-Kidd and Kiem, 2009). The Murray Basin, the East Coast and the Wet Tropics, all had strong reductions in both cool- and warm-season rainfall of similar magnitude, about 70 % below the long-term mean. In some regions, the Federation Drought was a strong warm-season feature (Central Slopes) while in the
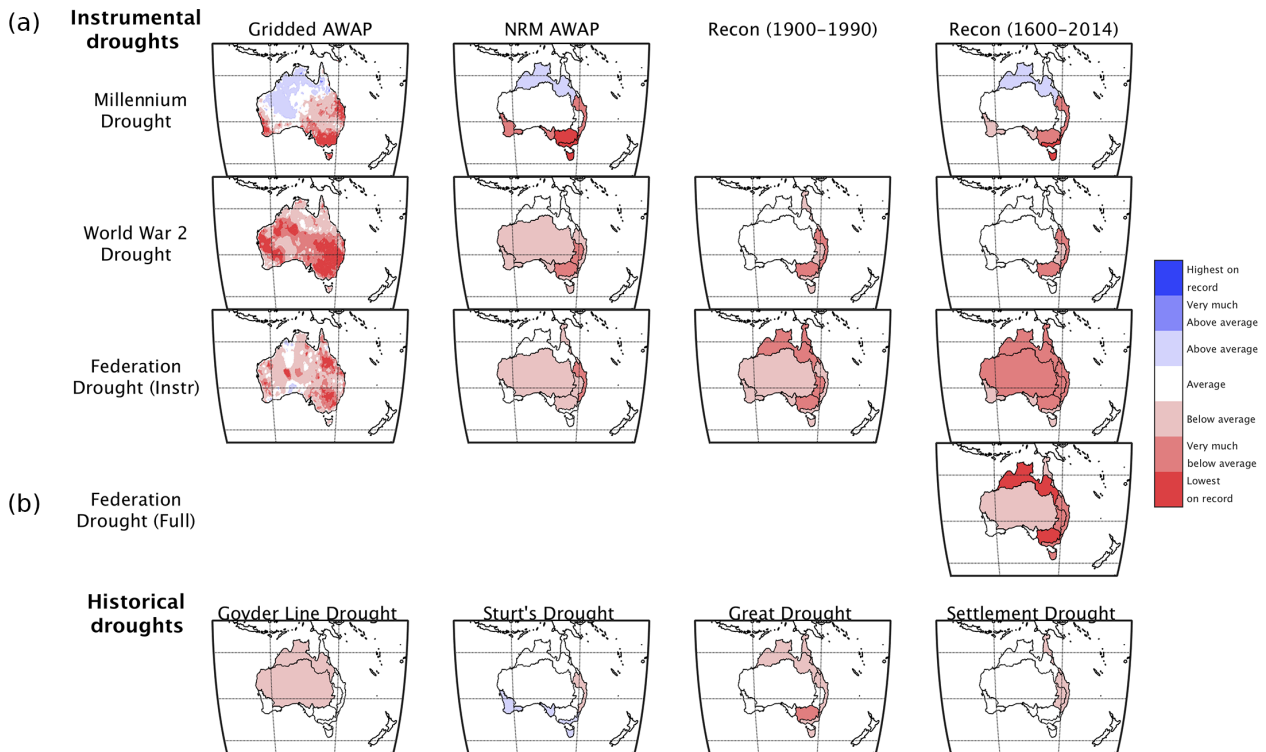
Figure 7. Annual deciles for major droughts. Plots for **(a)** Significant drought periods (according to Table 1c) during the instrumental period. Rankings of drought intensity are shown for three major instrumental period droughts. Column 1: AWAP gridded rainfall (1900–2014); column 2: NRM clusters (1900–2014); column 3: regional reconstructions during instrumental period (1900–1990); column 4: regional reconstructions during a four-century period (1600–2014). **(b)** Rankings of major drought periods during the reconstruction period (1600–2014).

tropical regions (Wet Tropics and Monsoonal North), rainfall reached remarkably low values. The intensity of the Federation Drought during the first few years seems to be a result of re-occurring El Niño episodes at that time and highlights ENSO's different spatial effects on Australian rainfall (Ummenhofer et al., 2009). Droughts such as the Murray Basin Drought can be clearly identified as an extended warm-season drought, not only in the Murray Basin but also along the East Coast and the Rangelands. Periods of severe long-term rainfall reductions highlight the spatial complexity of rainfall variability. There was abnormally low rainfall during the Southeast Australia Drought over an extended period of up to 10 years (Monsoonal North, Murray Basin, Southern and Southwestern Flatlands). This reduction was clearly a warm-season feature that was most severe along the East Coast and the Central Slopes. Sturt's Drought is another example of a spatially distinct localised warm-season drought in southeastern Australia that was also expressed as a long cool-season drought in the Rangelands. One of the strongest short-term drought episodes was the Black Thursday Drought in which warm-season rainfall was 60 % below the long-term average and cool-season rainfall was 30 % below the long-term mean. These deficits are likely to have contributed to the severe bushfires in 1851.

4.3.4 Extreme years in a long-term context

Severe short-term reductions of rainfall leading to events like the Black Thursday bushfires make clear the devastating effects that single extreme seasons can have. Our seasonally resolved reconstruction provides for the first time the opportunity to assess not only extreme years, but to assess individual extreme seasons.

Existing annually resolved reconstructions are likely to exhibit a specific seasonal bias, which may dilute the impacts of bi-seasonal effects across the year. Seasonal windows of drought indices often exhibit an integrated signal from multiple months to possibly years (Keyantash and Dracup, 2002). The rainfall reconstructions presented in this study enable us to identify temporally finer-scale extreme seasons of above/below rainfall. We identified the driest and wettest seasons for our regions by selecting the 10 strongest events using the instrumental (1900–2014) and reconstruction (1600–2014) periods.

Extreme years identified during the instrumental period reveal regional dependencies and differentiated seasonal aspects of dry and wet years (Table 2). In the pre-instrumental period similar patterns of spatially widespread extreme conditions in multiple regions occur (e.g. extreme dry 1481,
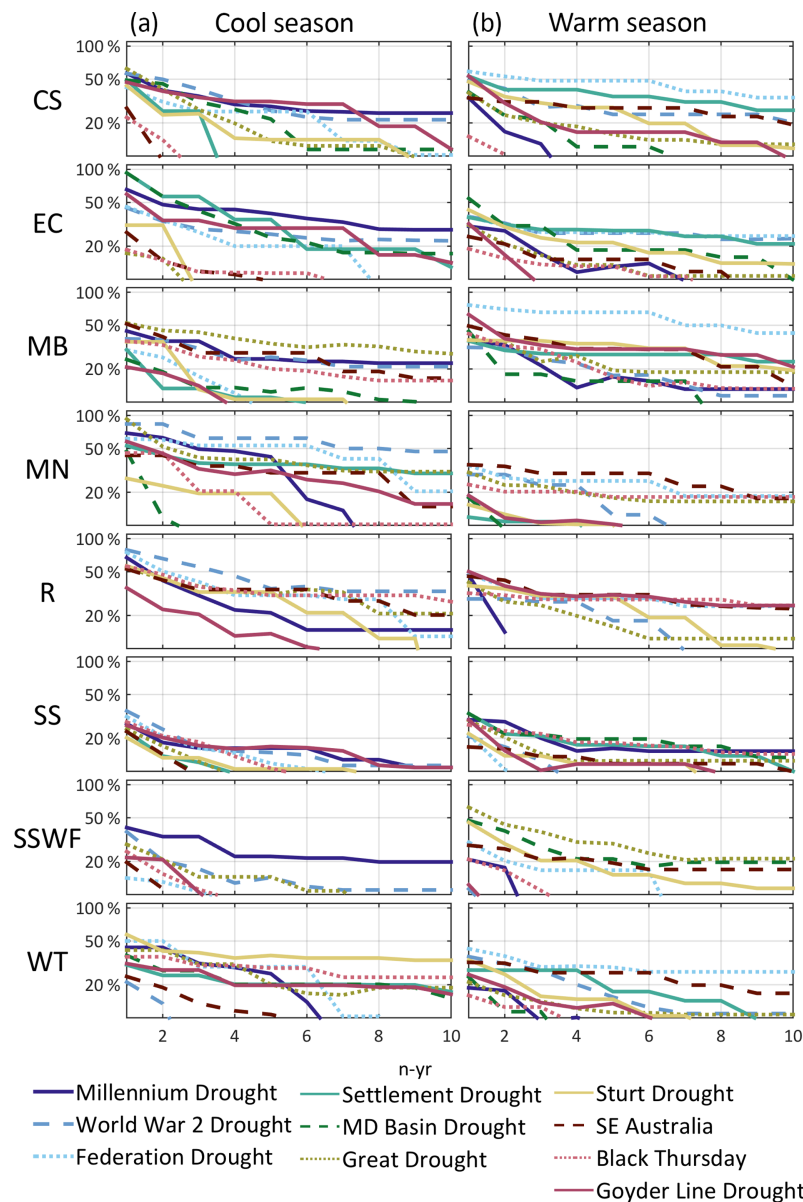
Figure 8. Rainfall drought depth duration percentages across the regions. The percentage reduction below the long-term average of the driest years of variable duration (1–10 years) within the selected drought periods, for the cool season **(a)** and warm season **(b)**.

1607, 1760 and 1817 (cool season), extreme wet 1759, 1826, 1871 and 1879 (cool season)). Conditions affecting multiple regions with similar magnitudes were rarer for wet than dry extremes. Warm-season rainfall during the first half of the 18th century (1720, 1731, 1732, 1740, 1752) was wettest across multiple regions, while dry conditions of similar magnitude occurred most frequently during the latter half of the 18th century (1761, 1760, 1814), affecting the East Coast, Southern Slopes and the Southwestern Flatlands.

The intensity of widespread extreme conditions such as 2010/2011 (wet) or 1982/1983 (dry) is much reduced during the pre-instrumental period. Based on our reconstructions

pre-instrumental seasons with an amplitude comparable to the 2010 pluvial include 1759 (East Coast) or 1826 (Central Slopes) and were only extreme across a few regions. Seasonally explicit extremes highlight the value of the finer temporal resolution resolved by these reconstructions. In 1833, East Coast reconstructed rainfall shows extreme dry conditions during the cool season followed by extremely wet conditions in the following warm season.

4.4 Comparing our reconstruction with other studies

Here we compare our results with published studies based on palaeo-records and early documentary compilations. We be-
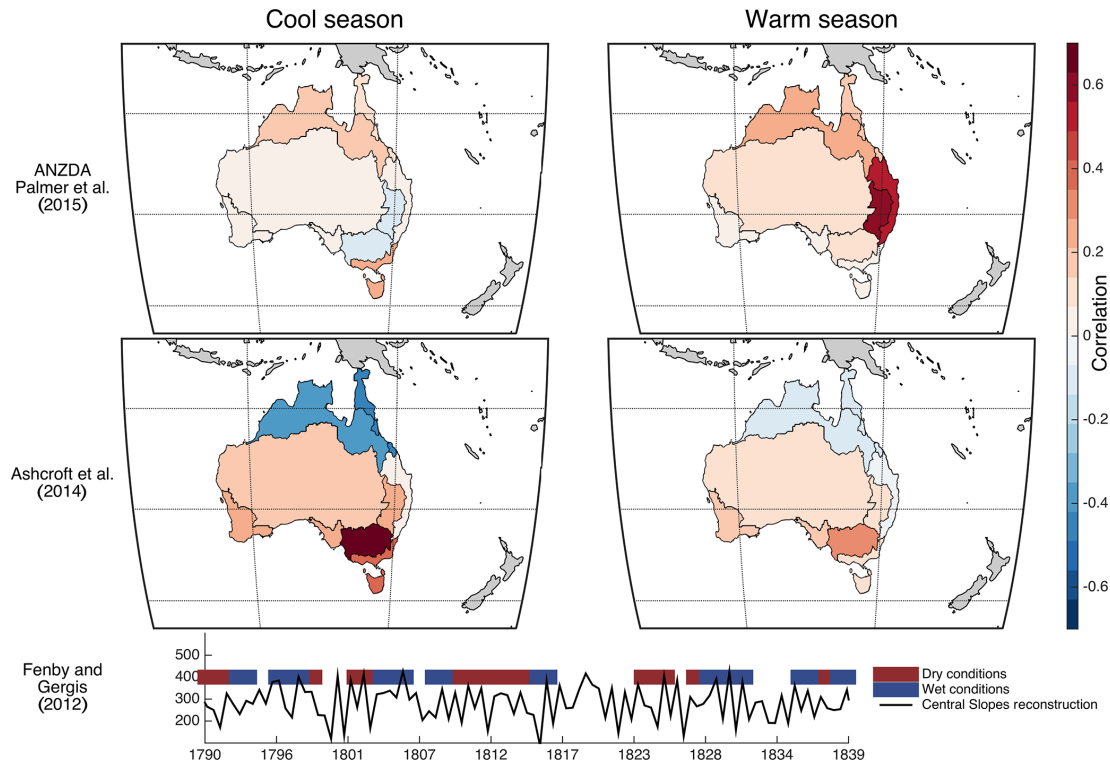
Figure 9. Comparison with published studies. Spatial correlation plot of regional NRM rainfall reconstruction and published studies on drought and rainfall. Spatial maps show region-wise correlation with the summer Australia New Zealand Drought Atlas (ANZDA) prior to the instrumental period (1600–1899) (Palmer et al., 2015), season-wise correlation with high-quality observational data from southeast Australia (Ashcroft et al., 2014) from 1832 to 1859 and a quantitative/visual comparison with pre-instrumental documentary sources compiled by (Fenby and Gergis, 2012) for southeast Australia (Central Slopes reconstruction from this study).

gin by comparing our results to the first spatially resolved reconstruction of Australian and New Zealand summer drought variability, the ANZDA (Palmer et al., 2015). As there is significant overlap in proxy records used in this study ($\sim 60\%$) and in Palmer et al. (2015), the two studies are not independent in their source data. Nevertheless, ANZDA is based on tree-ring records and a single coral record (which is not seasonally resolved), whereas our reconstruction includes seasonally resolved corals, as well as speleothem and ice-core records. In addition, the ANZDA differs substantially in its temporal (DJF) and spatial resolution, since it is a point-by-point gridded reconstruction, mostly verified for eastern Australia. The ANZDA also targets the PDSI, which is based not only on rainfall but also temperature and includes memory effects that account for soil moisture. The PDSI is therefore more likely to reflect agricultural droughts than meteorological droughts observed in rainfall. Figure 9 shows the correlations not accounting for memory effects between the warm-season (DJF) PDSI reconstruction (ANZDA) with our cool- and warm-season rainfall reconstructions. Non-significant correlations during the cool season and highly significant warm-season correlations, of up to 0.67 for the East Coast region, highlight agreement between our seasonal reconstruction and the summer season hydroclimatic features

detected by the PDSI reconstruction. Correlations with the summer season also reiterate the highly seasonal nature of ANZDA and its bias (intentional) towards only warm-season drought compared with our reconstructions. The strong temperature dependence of PDSI may explain some of the differences inland and why large parts of central Australia and all of Western Australia were not resolved by the ANZDA reconstruction.

The study by Ashcroft et al. (2014) details early documentary records of fine temporal resolution across southeastern Australia that are entirely independent of the data used in this study. The temporal coverage of the documentary records, however, is often less than 30 years. Nevertheless, there are strong positive correlations between the documentary-based record and the rainfall reconstruction for both the warm and cool seasons over the period 1832–1859 (Fig. 9). There are positive correlations between these records and our rainfall reconstructions across large areas in southeastern Australia, especially the Murray Basin (cool season). Figure 9 also shows a comparison of our reconstructions with rainfall variability as recorded in 18th–19th century (1788–1860) records from the populated coastal centres (Ashcroft et al., 2014; Fenby and Gergis, 2012). Years classified by Fenby and Gergis (2012) as dry or wet conditions are partially re-

flected in our Central Slopes reconstruction. The years 1790–1793, 1810–1813, and 1836–1837 are consistently classified as dry years, whereas 1788, 1806 and 1830 coincide with years classified as wet. Consecutive years of dry conditions from 1820–1828 appear to coincide, but single years such as 1801 and 1802 appear to be not in agreement with our reconstruction. This may be the result of more localised rainfall variability than is resolved by our regional Central Slopes reconstruction. Discrepancies between our reconstruction and documentary sources might also arise from the use of annual means, which might dilute a seasonal signal. Comparing annual means of our seasonal reconstructions (not shown) extreme years such as 1860 (East Coast) stand out and mostly agree with the wet and dry classified years found by Gergis and Ashcroft (2012) for southeast Australia.

5   Discussion and conclusions

In this study we used an extensive palaeo-climate proxy network derived from tree rings, corals, ice cores, and speleothem records to reconstruct precipitation in the eight NRM regions across Australia. This is the first Australia-wide reconstruction of seasonal rainfall extending ∼ 400 years into the past. The relationships between climate process indices were evaluated for the strength and stability of their relationship with precipitation in each NRM region for both the warm and cool seasons. We simultaneously assessed the strength and stability of relationships between individual proxy records and these same processes. This process-based approach enabled the reconstruction of precipitation based on teleconnections with major processes known to be related to Australian rainfall (Hendon et al., 2007; Risbey et al., 2009). The screening of predictors based on the strength and stability of their relationship with the climate indices constrains the inclusion of predictors during the instrumental period but still relies on a continuing stationarity assumption on multidecadal timescales. All reconstructions successfully verified over the 1749–1984 period, and many back to the early 16th century. A comparison with the ANZDA reconstruction showed a high level of agreement with eastern Australian drought conditions during the warm season. Independent high-resolution early documentary records by Ashcroft et al. (2014) compared well with the cool- and warm-season reconstructions. It should be pointed out that our seasonal reconstructions represent rainfall only. Droughts are a result of complex interactions of various atmospheric variables and interactions at different timescales. Important factors contributing to droughts are temperature, soil moisture and evaporation, which are not accounted for in this reconstruction. We also assessed extreme years of high and low rainfall with published documentary sources. A majority of years previously identified as having anomalously high or low rainfall events agree well with our seasonal reconstructions. Most of those comparisons are con-

fined to southeastern Australia due to regional biases in documentary records. Nevertheless, these additional verification approaches highlight the quality of our seasonal reconstruction and its ability to represent past rainfall variability.

On decadal to multi-decadal timescales, substantial low-frequency variability is present across the regions and seasons. An investigation of recent trends revealed evidence for unusual tendencies towards wetter conditions in the north in the warm season and drier conditions in the south in the cool season. Northern regions (Monsoonal North, Wet Tropics) have experienced an increase over the last 30–50 years in rainfall, predominantly during the warm (wet) season (Nicholls, 2006; Taschetto and England, 2009), when the majority of rainfall occurs. The significance of this increase is difficult to determine due to high intrinsic variability in the tropical north. The extended baseline of our reconstruction helps to place these changes into a long-term context. In particular, after the 1970s the increase of warm-season rainfall in the Monsoonal North (and the Rangelands) is highly unusual relative to past centuries. Possible mechanisms could be strengthening of the monsoon modulated by the ENSO conditions in the western Pacific (Fig. 2), intensification and shifts in deep convection related to the monsoon trough (Taschetto and England, 2009), and anthropogenic forcing enhancing rainfall and cloud formation (Cai et al., 2014). Possible enhancement of atmospheric pressure systems over the Indian Ocean in conjunction with a strengthening of SAM (Feng et al., 2013) is a further possibility. From the correlation analysis of possible drivers (Fig. 2) neither the IOD nor SAM are significantly correlated with rainfall in the northern regions, so this latter possibility seems unlikely.

The tendency towards drier conditions in southern Australia is less clear. Our analysis showed that the most recent decline in rainfall in the Southern Slopes is within the range of variability given by the reconstruction. The cool-season decline in the south is often associated with the intensification of the subtropical ridge (Timbal and Drosdowsky, 2012; Timbal et al., 2006), changes in large-scale atmospheric circulation such as the Indian Ocean (Ummenhofer et al., 2011), and the observed upward trend in SAM (Cai and Cowan, 2006). All of these processes are significantly linked to interannual rainfall variability in the south (Fig. 2) but are not particularly unusual in terms of natural variability resolved by the reconstruction. Strong decadal to multidecadal variability can be observed across all of the regions that account for declines similar to the most recently observed trends. At least in terms of 30- to 50-year trend periods, the declining trends are within the range of intrinsic reconstructed variability. The declining trend of rainfall during the cool season is particularly strong in the Murray Basin. The most recent trends starting after 1950s and 1970s are not unprecedented but are below the 25th percentile, pointing towards a drying tendency. Further work could specifically focus on the long-term declining trend for the cool season in south and southwestern Australia (Fig. 6) observed since around 1910.

In order to assess the severity of droughts in a long-term context, reconstructions need to be consistent with the representation of droughts in the instrumental record. All three major droughts during the instrumental periods are well represented in terms of their spatial extent, intensity and duration considering the reduced spatial representation of regional averages (Fig. 7) (cf. Verdon-Kidd and Kiem, 2009). The three protracted droughts remain severe when considered in the ∼ 400-year context provided by our reconstructions, especially in south and southeastern Australia. Although all three droughts have very distinct spatial footprints, the spatial extent and concurrent drought conditions across broad areas are quite unique compared to historical droughts. The Millennium Drought stands out as an unprecedented drought in the Southern Slopes region (Fig. 7). The World War II Drought seems not to be as exceptional when considering the full reconstruction period back to 1600; only central and eastern regions were very much below average. The Federation Drought, which was mostly prior to the observational period, is confirmed as one of the worst periods of suppressed rainfall in the Murray Basin and the Monsoonal North region. Compared to droughts during the longer period, these three major droughts affected large parts of Australia, whereas pre-instrumental drought episodes such as the Great Drought appeared to be much more regionally constrained.

The record breaking wet years 2010–2011 accompanied by the strong La Niña episode were extreme during the warm season across all regions. During that time the Murray Darling Basin had the largest rainfall anomalies since 1900 (CSIRO, 2012). In the much longer context of our rainfall reconstruction, 2010–2011 was one of the wettest warm seasons in the past several centuries, not only in Murray Basin but also in Monsoonal North, Rangelands, Southern Slopes and East Coast. Cook et al. (2016) found similar results based on the ANZDA reconstruction of spatial variability in the PDSI. The 1979–1983 period of dry conditions in eastern Australia and the 1983 warm season and 1984 cool-season wet anomalies in the East Coast, Wet Tropics and Monsoonal North are also captured in the reconstructions. The consecutive 1927 (cool), 1928 (warm) and 1928 (cool) seasons experienced extremely dry conditions in the Central Slopes region. Interestingly, extreme cool- and warm-season wet conditions affected multiple regions, while extreme dry conditions appear to have occurred more often in single regions. This relationship persists into the pre-instrumental period. The known asymmetry of the different ENSO phases impacting Australian rainfall could explain those differences (Cai et al., 2012). While El Niño-induced rainfall reductions are not related to the event amplitude, the La Niña phase of ENSO produces more extreme pluvial events. This is consistent with observations that La Niña is more strongly teleconnected to rainfall and hence extreme rainfall events (Cai et al., 2010; King et al., 2013) than El Niño events are to rainfall deficit.

The spatial extent of various droughts and pluvial episodes may help to identify the specific drivers behind the individual events. For 20th century droughts, the interaction of climate modes and anthropogenic warming may have played a significant role in the drought episodes (Cai et al., 2014). However, the longer historical perspective provided by our rainfall reconstructions could help to attribute those factors in further studies by considering individual climate modes and their interactions.

New insights about drought characteristics are derived from the comparison of instrumental and historical droughts of different duration. Independent palaeoclimate reconstructions could help to relate the rainfall variability back to the climatic drivers causing these diverse drought characteristics in terms of their spatial and temporal characteristics and could provide important insights into the climate modes. Different contributing processes are difficult to examine with only a few events during the instrumental period. Droughts confined to a specific season can be distinct and classified by intensity, extent and duration. Again, the three major drought events during the instrumental period stand out in terms of their intensity and number of regions affected. The Millennium Drought as a cool-season feature and the Federation Drought as a warm-season feature clearly highlight the merits of a seasonally resolved reconstructions (Fig. 8). Another example is the Southeast Australia Drought, which had persistent dry conditions during the warm season for up to 10 years.

Natural variability and, in particular, the low-frequency contributions from decadal modes such as the IPO could contribute to those dry conditions in various ways. Additional realisations of multi-year droughts can help to understand physical mechanisms that lead to dry conditions, untangle dynamical interactions of various climatic modes, and lead to a better understanding of future drought risks. Inverse approaches and additional palaeoclimate reconstructions could help to deduce the climatic drivers causing these diverse drought characteristics and could provide important insights into the climate modes, their interactions, and influences on Australian droughts and pluvials. Our multi-century, bi-seasonal and spatially resolved reconstructions provide new opportunities to study the dynamics of meteorological droughts across the Australian continent. For example, do similar settings such as a positive IOD, a positive ENSO, and a positive IPO lead to similar impacts on Australian droughts? It is imperative that we answer questions like this due to Australia's significant vulnerability to prolonged drought episodes. Future work should consider further subdivision to resolve finer-scale hydroclimatic patterns important for regional assessments. This could include a subdivision of large regions such as the Rangelands and regions of complex rainfall regimes like Tasmania as suggested by the NRM sub-clusters (CSIRO and Bureau of Meteorology, 2015).

References

Allan, R. J. and Haylock, M. R.: Circulation features associated with the winter rainfall decrease in Southwestern Australia, J. Climate, 6, 1356–1367, 1993.

Allen, K. J., Lee, G., Ling, F., Allie, S., Willis, M., and Baker, P. J.: Palaeohydrology in climatological context: developing the case for use of remote predictors in Australian streamflow reconstructions, Appl. Geogr., 64, 132–152, https://doi.org/10.1016/j.apgeog.2015.09.007, 2015.

Ashcroft, L., Gergis, J., and Karoly, D. J.: A historical climate dataset for southeastern Australia, 1788–1859, Geosci. Data J., 1, 158–178, https://doi.org/10.1002/gdj3.19, 2014.

Ashok, K., Behera, S. K., Rao, S. A., Weng, H., and Yamagata, T.: El Niño Modoki and its possible teleconnection, J. Geophys. Res.-Oceans, 112, C11007, https://doi.org/10.1029/2006JC003798, 2007.

Bradley, R. S. and Jonest, P. D.: "Little Ice Age" summer temperature variations: their nature and relevance to recent global warming trends, Holocene, 3, 367–376, https://doi.org/10.1177/095968369300300409, 1993.

Cai, W. and Cowan, T.: SAM and regional rainfall in IPCC AR4 models: can anthropogenic forcing account for southwest Western Australian winter rainfall reduction?, Geophys. Res. Lett., 33, L24708, https://doi.org/10.1029/2006GL028037, 2006.

Cai, W. and Cowan, T.: Dynamics of late autumn rainfall reduction over southeastern Australia, Geophys. Res. Lett., 35, L09708, https://doi.org/10.1029/2008GL033727, 2008.

Cai, W., van Rensch, P., Cowan, T., and Sullivan, A.: Asymmetry in ENSO teleconnection with regional rainfall, its multidecadal variability, and impact, J. Climate, 23, 4944–4955, https://doi.org/10.1175/2010JCLI3501.1, 2010.

Cai, W., van Rensch, P., Cowan, T., and Hendon, H. H.: An asymmetry in the IOD and ENSO teleconnection pathway and its impact on Australian climate, J. Climate, 25, 6318–6329, https://doi.org/10.1175/JCLI-D-11-00501.1, 2012.

Cai, W., Purich, A., Cowan, T., van Rensch, P., and Weller, E.: Did climate change-induced rainfall trends contribute to the Australian Millennium Drought?, J. Climate, 27, 3145–3168, https://doi.org/10.1175/JCLI-D-13-00322.1, 2014.

Cook, B. I., Ault, T. R., and Smerdon, J. E.: Unprecedented 21st century drought risk in the American Southwest and Central Plains, Sci. Adv., 1, e1400082, https://doi.org/10.1126/sciadv.1400082, 2015.

Cook, B. I., Palmer, J. G., Cook, E. R., Turney, C. S. M., Allen, K., Fenwick, P., O'Donnell, A., Lough, J. M., Grierson, P. F., Ho, M., and Baker, P. J.: The paleoclimate context and future trajectory of extreme summer hydroclimate in eastern Australia, J. Geophys. Res.-Atmos., 121, 12820–12838, https://doi.org/10.1002/2016JD024892, 2016.

Cook, E. R., Briffa, K. R., and Jones, P. D.: Spatial regression methods in dendroclimatology: a review and comparison of two techniques, Int. J. Climatol., 14, 379–402, 1994.

Cook, E. R., Anchukaitis, K. J., Buckley, B. M., D'Arrigo, R. D., Jacoby, G. C., and Wright, W. E.: Asian Monsoon Failure and Megadrought During the Last Millennium, Science, 328, 486–489, https://doi.org/10.1126/science.1185188, 2010.

Cook, E. R., Seager, R., Kushnir, Y., Briffa, K. R., Büntgen, U., Frank, D., Krusic, P. J., Tegel, W., Van der Schrier, G., Andreu-Hayles, L., Baillie, M., Baittinger, C., Bleicher, N., Bonde, N., Brown, D., Carrer, M., Cooper, R., Čufar, K., Dittmar, C., Esper, J., Griggs, C., Gunnarson, B., Günther, B., Gutierrez, E., Haneca, K., Helama, S., Herzig, F., Heussner, K. U., Hofmann, J., Janda, P., Kontic, R., Köse, N., Kyncl, T., Levanič, T., Linderholm, H., Manning, S., Melvin, T. M., Miles, D., Neuwirth, B., Nicolussi, K., Nola, P., Panayotov, M., Popa, I., Rothe, A., Seftigen, K., Seim, A., Svarva, H., Svoboda, M., Thun, T., Timonen, M., Touchan, R., Trotsiuk, V., Trouet, V., Walder, F., Ważny, T., Wilson, R., and Zang, C.: Old World megadroughts and pluvials during the Common Era, Sci. Adv., 1, e1500561, https://doi.org/10.1126/sciadv.1500561, 2015.

CSIRO: Climate and water availability in southeastern Australia: a synthesis of findings from Phase 2 of the South Eastern Australian Climate Initiative (SEACI), CSIRO, Canberra, available at: http://www.seaci.org (last access: 28 February 2017), 2012.

CSIRO and Bureau of Meteorology: Climate Change in Australia Information for Australia's Natural Resource Management Regions: Technical Report, CSIRO and Bureau of Meteorology, Australia, 2015.

Cullen, L. E. and Grierson, P. F.: Multi-decadal scale variability in autumn-winter rainfall in south-western Australia since 1655 AD as reconstructed from tree rings of Callitris columellaris, Clim. Dynam., 33, 433–444, https://doi.org/10.1007/s00382-008-0457-8, 2008.

Drosdowsky, W.: An analysis of Australian seasonal rainfall anomalies – 1950–1987. 2. Temporal variability and teleconnection patterns, Int. J. Climatol., 13, 111–149, 1993.

Fenby, C. and Gergis, J.: Rainfall variations in south-eastern Australia part 1: consolidating evidence from pre-instrumental documentary sources, 1788–1860, Int. J. Climatol., 33, 2956–2972, https://doi.org/10.1002/joc.3640, 2012.

Feng, J., Li, J., and Xu, H.: Increased summer rainfall in northwest Australia linked to southern Indian Ocean climate variability, J. Geophys. Res.-Atmos., 118, 467–480, https://doi.org/10.1029/2012JD018323, 2013.

Fiddes, S. and Timbal, B.: Future impacts of climate change on streamflows across Victoria, Australia: making use of statistical downscaling, Clim. Res., 71, 219–236, https://doi.org/10.3354/cr01447, 2017.

Freund, M.: Multi-century cool and warm season rainfall reconstructions for Australia's major climatic regions: Data and additional information on a seasonal rainfall reconstruction of major NRM regions based on paleoclimate data, https://doi.org/10.4225/49/59e3ee30cdbbc, 2017.

Gallant, A., Phipps, S. J., and Karoly, D. J.: Nonstationary Australasian teleconnections and implications for paleoclimate reconstructions, J. Climate, 26, 8827–8849, https://doi.org/10.1175/JCLI-D-12-00338.1, 2013.

Gallant, A. J. E. and Gergis, J.: An experimental streamflow reconstruction for the River Murray, Australia, 1783–1988, Water Resour. Res., 47, W00G04, https://doi.org/10.1029/2010WR009832, 2011.

Gergis, J. and Ashcroft, L.: Rainfall variations in south-eastern Australia part 2: a comparison of documentary, early instrumental and palaeoclimate records, 1788–2008, Int. J. Climatol., 33, 2973–2987, https://doi.org/10.1002/joc.3639, 2012.

Gergis, J., Garden, D., and Fenby, C.: The influence of climate on the first european settlement of Australia: a comparison of weather journals, documentary data and palaeoclimate records, 1788–1793, Environ. Hist., 15, 485–507, https://doi.org/10.1093/envhis/emq079, 2010.

Gergis, J., Gallant, A. J. E., Braganza, K., Karoly, D. J., Allen, K., Cullen, L., D'Arrigo, R., Goodwin, I., Grierson, P., and McGregor, S.: On the long-term context of the 1997–2009 "Big Dry" in South-Eastern Australia: insights from a 206-year multi-proxy rainfall reconstruction, Clim. Change, 111, 923–944, https://doi.org/10.1007/s10584-011-0263-x, 2011.

Heinrich, I., Weidner, K., Helle, G., Vos, H., Lindesay, J., and Banks, J. C. G.: Interdecadal modulation of the relationship between ENSO, IPO and precipitation: insights from tree rings in Australia, Clim. Dynam., 33, 63–73, https://doi.org/10.1007/s00382-009-0544-5, 2009.

Helman, P.: Droughts in the Murray–Darling Basin Since European Settlement, Griffith University, Southport, 2009.

Hendon, H. H., Thompson, D. W. J., and Wheeler, M. C.: Australian rainfall and surface temperature variations associated with the Southern Hemisphere annular mode, J. Climate, 20, 2452–2467, https://doi.org/10.1175/JCLI4134.1, 2007.

Henley, B. J., Gergis, J., Karoly, D. J., Power, S., Kennedy, J., and Folland, C. K.: A tripole index for the Interdecadal Pacific Oscillation, Clim. Dynam., 45, 1–14, https://doi.org/10.1007/s00382-015-2525-1, 2015.

Henley, B. J., Meehl, G., Power, S. B., Folland, C. K., King, A. D., Brown, J. N., Karoly, D. J., Delage, F., Gallant, A. J. E., Freund, M., and Neukom, R.: Spatial and temporal agreement in climate model simulations of the Interdecadal Pacific Oscillation, Environ. Res. Lett., 12, 044011, https://doi.org/10.1088/1748-9326/aa5cc8, 2017.

Hope, P., Timbal, B., and Fawcett, R.: Associations between rainfall variability in the southwest and southeast of Australia and their evolution through time, Int. J. Climatol., 30, 1360–1371, https://doi.org/10.1002/joc.1964, 2009.

Hutchinson, M. F.: Interpolating mean rainfall using thin plate smoothing splines, Int. J. Geogr. Inf. Syst., 9, 385–403, https://doi.org/10.1080/02693799508902045, 1995.

Jones, D. A., Wang, W., and Fawcett, R.: High-quality spatial climate data-sets for Australia, Aust. Meteorol. Ocean., 58, 233–248, 2009.

Keyantash, J. and Dracup, J. A.: The quantification of drought: an evaluation of drought indices, B. Am. Meteorol. Soc., 83, 1167–1180, 2002.

King, A. D., Alexander, L. V., and Donat, M. G.: Asymmetry in the response of eastern Australia extreme rainfall to low-frequency Pacific variability, Geophys. Res. Lett., 40, 2271–2277, https://doi.org/10.1002/grl.50427, 2013.

Koch, S. E., Desjardins, M., and Kocin, P. J.: An interactive barnes objective map analysis scheme for use with satellite and conventional data, J. Clim. Appl. Meteorol., 22, 1487–1503, 1983.

Larsen, S. H. and Nicholls, N.: Southern Australian rainfall and the subtropical ridge: variations, interrelationships, and trends, Geophys. Res. Lett., 36, L08708, https://doi.org/10.1029/2009GL037786, 2009.

Lough, J. M., Lewis, S. E., and Cantin, N. E.: Freshwater impacts in the central Great Barrier Reef: 1648–2011, Coral Reefs, 34, 739–751, https://doi.org/10.1007/s00338-015-1297-8, 2015.

Maher, P. and Sherwood, S. C.: Disentangling the multiple sources of large-scale variability in Australian wintertime precipitation, J. Climate, 27, 6377–6392, https://doi.org/10.1175/JCLI-D-13-00659.1, 2014.

Marshall, G.: AMS Journals Online – trends in the Southern Annular Mode from observations and reanalyses, J. Climate, 16, 4134–4143, 2003.

McBride, J. L. and Nicholls, N.: Seasonal relationships between Australian rainfall and the Southern Oscillation, Mon. Weather Rev., 111, 1998–2004, 1983.

Melvin, T. M. and Briffa, K. R.: A signal-free approach to dendroclimatic standardisation, Dendrochronologia, 26, 71–86, https://doi.org/10.1016/j.dendro.2007.12.001, 2008.

Murphy, B. F. and Timbal, B.: A review of recent climate variability and climate change in southeastern Australia, Int. J. Climatol., 28, 859–879, https://doi.org/10.1002/joc.1627, 2008.

Neukom, R. and Gergis, J.: Southern Hemisphere high-resolution palaeoclimate records of the last 2000 years, Holocene, 22, 501–524, https://doi.org/10.1177/0959683611427335, 2012.

Nicholls, N.: Detecting and attributing Australian climate change: a review, Aust. Meteorol. Mag., 55, 199–211, 2006.

Nicholls, N., Drosdowsky, W., and Lavery, B.: Australian rainfall variability and change, Weather, 52, 66–72, https://doi.org/10.1002/j.1477-8696.1997.tb06274.x, 1997.

Oliveira, F. N. M. and Ambrizzi, T.: The effects of ENSO-types and SAM on the large-scale southern blockings, Int. J. Climatol., 37, 3067–3081, https://doi.org/10.1002/joc.4899, 2016.

Palmer, J. G., Cook, E. R., Turney, C. S. M., Allen, K., Fenwick, P., Cook, B. I., O'Donnell, A., Lough, J., Grierson, P., and Baker, P.: Drought variability in the eastern Australia and New Zealand summer drought atlas (ANZDA, CE 1500–2012) modulated by the Interdecadal Pacific Oscillation, Environ. Res. Lett., 10, 1–12, https://doi.org/10.1088/1748-9326/10/12/124002, 2015.

Pook, M. and Gibson, T.: Atmospheric blocking and storm tracks during SOP-1 of the FROST Project, Aust. Meteorol. Mag., 1, 51–60, 1999.

Ren, H.-L. and Jin, F.-F.: Niño indices for two types of ENSO, Geophys. Res. Lett., 38, L04704, https://doi.org/10.1029/2010GL046031, 2011.

Risbey, J. S., Pook, M. J., and McIntosh, P. C.: On the remote drivers of rainfall variability in Australia, Mon. Weather Rev., 137, 3233–3253, https://doi.org/10.1175/2009MWR2861.1, 2009.

Saji, N. H., Goswami, B. N., and Vinayachandran, P. N.: A dipole mode in the tropical Indian Ocean, Nature, 401, 360–363, https://doi.org/10.1038/43854, 1999.

Smith, I.: An assessment of recent trends in Australian rainfall, Aust. Meteorol. Mag., 53, 163–173, 2004.

Speer, M. S., Leslie, L. M., and Fierro, A. O.: Australian east coast rainfall decline related to large scale climate drivers, Clim. Dynam., 36, 1419–1429, https://doi.org/10.1007/s00382-009-0726-1, 2009.

Taschetto, A. S. and England, M. H.: An analysis of late twentieth century trends in Australian rainfall, Int. J. Climatol., 29, 791–807, https://doi.org/10.1002/joc.1736, 2009.

Tierney, J. E., Abram, N. J., Anchukaitis, K. J., Evans, M. N., Giry, C., Kilbourne, K. H., Saenger, C. P., Wu, H. C., and Zinke, J.: Tropical sea surface temperatures for the past four centuries reconstructed from coral archives, Paleoceanography, 30, 226–252, 2015.

Timbal, B. and Drosdowsky, W.: The relationship between the decline of Southeastern Australian rainfall and the strengthening of the subtropical ridge, Int. J. Climatol., 33, 1021–1034, https://doi.org/10.1002/joc.3492, 2012.

Timbal, B. and Fawcett, R.: A historical perspective on southeastern Australian rainfall since 1865 using the instrumental record, J. Climate, 26, 1112–1129, https://doi.org/10.1175/JCLI-D-12-00082.1, 2013.

Timbal, B., Arblaster, J. M., and Power, S.: Attribution of the late-twentieth-century rainfall decline in southwest Australia, J. Climate, 19, 2046–2062, 2006.

Tozer, C. R., Vance, T. R., Roberts, J. L., Kiem, A. S., Curran, M. A. J., and Moy, A. D.: An ice core derived 1013-year catchment-scale annual rainfall reconstruction in subtropical eastern Australia, Hydrol. Earth Syst. Sci., 20, 1703–1717, https://doi.org/10.5194/hess-20-1703-2016, 2016.

Ummenhofer, C. C., England, M. H., McIntosh, P. C., Meyers, G. A., Pook, M. J., Risbey, J. S., Gupta, A. S., and Taschetto, A. S.: What causes southeast Australia's worst droughts?, Geophys. Res. Lett., 36, L04706, https://doi.org/10.1029/2008GL036801, 2009.

Ummenhofer, C. C., Gupta, Sen, A., Briggs, P. R., England, M. H., McIntosh, P. C., Meyers, G. A., Pook, M. J., Raupach, M. R., and Risbey, J. S.: Indian and Pacific Ocean influences on Southeast Australian drought and soil moisture, J. Climate, 24, 1313–1336, https://doi.org/10.1175/2010JCLI3475.1, 2011.

Vance, T. R., Roberts, J. L., Plummer, C. T., Kiem, A. S., and van Ommen, T. D.: Interdecadal Pacific variability and eastern Australian megadroughts over the last millennium, Geophys. Res. Lett., 42, 129–137, https://doi.org/10.1002/2014GL062447, 2015.

van Dijk, A. I. J. M., Beck, H. E., Crosbie, R. S., de Jeu, R. A. M., Liu, Y. Y., Podger, G. M., Timbal, B., and Viney, N. R.: The Millennium Drought in southeast Australia (2001–2009): natural and human causes and implications for water resources, ecosystems, economy, and society, Water Resour. Res., 49, 1040–1057, https://doi.org/10.1002/wrcr.20123, 2013.

Verdon-Kidd, D. C. and Kiem, A. S.: Nature and causes of protracted droughts in southeast Australia: comparison between the Federation, WWII, and Big Dry droughts, Geophys. Res. Lett., 36, L22707, https://doi.org/10.1029/2009GL041067, 2009.

Wang, G. and Hendon, H. H.: Sensitivity of Australian Rainfall to Inter–El Niño Variations, J. Climate, 20, 4211–4226, https://doi.org/10.1175/JCLI4228.1, 2007.

Wardle, R.: Modeled response of the Australian monsoon to changes in land surface temperatures, Geophys. Res. Lett., 31, L16205, https://doi.org/10.1029/2004GL020157, 2004.

Watterson, I. G.: Components of precipitation and temperature anomalies and change associated with modes of the Southern Hemisphere, Int. J. Climatol., 29, 809–826, https://doi.org/10.1002/joc.1772, 2009.

Watterson, I. G.: Understanding and partitioning future climates for Australian regions from CMIP3 using ocean warming indices, Climatic Change, 111, 903–922, https://doi.org/10.1007/s10584-011-0166-x, 2011.